# Runoff Threshold Responses in Continental Boreal Catchments

Devito, K. J.; O'Sullivan, A. M.; Peters, D. L.; Hokanson, K. J.; Kettridge, N.; Mendoza, C. A.

*DOI:*
10.1029/2023WR034752

AGU ADVANCING EARTH AND SPACE SCIENCES

Water Resources Research®

RESEARCH ARTICLE
10.1029/2023WR034752

**Key Points:**

- Runoff threshold responses and magnitude of low and high flow vary between neighboring catchments receiving similar annual precipitation
- Four catchment runoff functional types are associated with contrasts in fine- versus coarse-textured substrates and peatland versus forest covers
- The influence of landscape heterogeneity on thresholds in annual runoff shifts dramatically with weather patterns

**Supporting Information:**

Supporting Information may be found in the online version of this article.

**Correspondence to:**
K. J. Devito,
kdevito@ualberta.ca

**Citation:**
Devito, K. J., O'Sullivan, A. M., Peters, D. L., Hokanson, K. J., Kettridge, N., & Mendoza, C. A. (2023). Runoff threshold responses in continental Boreal catchments: Nexus of subhumid climate, low-relief, surficial geology, and land cover. *Water Resources Research*, *59*, e2023WR034752. https://doi.org/10.1029/2023WR034752

Received 24 FEB 2023
Accepted 29 SEP 2023

**Author Contributions:**
**Conceptualization:** K. J. Devito, C. A. Mendoza
**Data curation:** K. J. Devito
**Formal analysis:** K. J. Devito, A. M. O'Sullivan, K. J. Hokanson
**Methodology:** K. J. Devito, A. M. O'Sullivan, D. L. Peters, K. J. Hokanson, N. Kettridge
**Resources:** K. J. Devito



# Runoff Threshold Responses in Continental Boreal Catchments: Nexus of Subhumid Climate, Low-Relief, Surficial Geology, and Land Cover

**K. J. Devito[1], A. M. O'Sullivan[2,3], D. L. Peters[4], K. J. Hokanson[5], N. Kettridge[1,6], and C. A. Mendoza[5]**

[1]Department of Biological Sciences, University of Alberta, Edmonton, AB, Canada, [2]O'Sullivan EcoHydraulics Inc., Fredericton, NB, Canada, [3]Faculty of Forestry and Environmental Management and Biology Department, Canadian Rivers Institute, University of New Brunswick, Fredericton, NB, Canada, [4]Environment and Climate Change Canada, University of Victoria Queenswood Campus, Victoria, BC, Canada, [5]Department of Earth and Atmospheric Sciences, University of Alberta, Edmonton, AB, Canada, [6]School of Geography, Earth and Environmental Sciences, University of Birmingham, Edgbaston, UK

**Abstract** We examined annual runoff from 20 meso-scale catchments over 25 years, to elucidate how interactions between physiography and long-term weather patterns influence the magnitude of spatial–temporal thresholds in annual runoff responses in water-limited, low-relief, glaciated continental Boreal landscapes. Annual runoff ranged over 2 orders of magnitude (<3 to >300 mm) among catchments receiving similar annual precipitation. Threshold relationships were observed with cumulative regional moisture deficits that reflected spatial–temporal differences in effective storage and antecedent moisture among catchments with differing portions of glacial-deposit and land-cover types. The importance of the glacial-deposit texture and forest-peatland cover on runoff behavior among catchments varied with weather patterns and catchment antecedent moisture states. Dry states yielded low annual runoff that ranged by 2 orders of magnitude (0–80 mm), with higher values in catchments with predominantly coarse-textured deposits. During near normal antecedent moisture, annual runoff remained low (<10 mm) in catchments associated with fine-textured, hummocky landforms and deciduous forests. Annual runoff >10 mm was observed only in catchments with extensive peatlands. Infrequent wet states resulted in increased runoff in all catchments; however, ranges in maximum runoff were associated with heterogeneity in catchment landforms and land covers. Integrating cumulative precipitation with the proportion of glacial-deposit and land-cover types within catchments can (a) represent water cycling and regional sink-source dynamics controlling runoff and (b) provide an effective management framework for predicting climate and land use impacts on regional runoff in water-limited, low-relief, glaciated landscapes such as the Boreal Plain.

## 1. Introduction

The hydrologic, physiographic, and climatic setting of an area imparts an appreciable control on the seasonality and magnitude of runoff (*R*) generation or threshold responses (Zehe & Sivapalan, 2009). Thresholds in runoff response refer to "critical moment(s) in time or position in space where the runoff behavior rapidly changes" (Ross et al., 2021).The hydro-physio-climatic setting of an area can influence the general catchment function as it controls the form and magnitude of precipitation (*P*) relative to vegetation demand, the soil storage, and aquifer interaction determining antecedent moisture conditions and therefore flow path and temporal and spatial changes in *R* with input *P* (Carey et al., 2010; Devito et al., 2005; McNamara et al., 2005). To this end, many researchers encourage intercatchment comparisons of runoff dynamics across a breadth of physical and climate characteristics (Ali et al., 2015; Julian & Gardner, 2014; McNamara et al., 2011). Such studies provide insights into the relative role and interaction of catchment heterogeneity with climate on storage (*S*) and *R* dynamics, while also allowing researchers to develop an awareness of how different landscapes may be resilient to environmental change (e.g., Ehsanzadeh et al., 2012; Pilgrim et al., 1988; Singh et al., 2014; Tetzlaff et al., 2009).

Intercatchment comparisons have increased our understanding of how topography (Dreps et al., 2014), soil pedology (Gannon et al., 2014; Lin et al., 2006; Testzlaff et al., 2014), and surficial or bedrock geology (Cowood et al., 2017; O'Sullivan et al., 2020; Pfister et al., 2017) interact with overlying vegetation to influence the spatial distribution of soil–groundwater *S* and catchment (antecedent) moisture states. These characteristics, in turn,

**Visualization:** K. J. Devito, A. M. O'Sullivan, D. L. Peters, N. Kettridge, C. A. Mendoza
**Writing – original draft:** K. J. Devito
**Writing – review & editing:** K. J. Devito, A. M. O'Sullivan, D. L. Peters, K. J. Hokanson, N. Kettridge, C. A. Mendoza

define differences or similarities in the memory of wetting and drying periods, and thus surface and subsurface hydrological connectivity, and the degree of nonlinearity or abruptness of the threshold response to current *P* events (Buttle & Eimers, 2009; McNamara et al., 2005; Nippgen et al., 2011). Integrated catchment characteristics also influence the potential for and proportion of hydrologically connected (direct) or disconnected (indirect) subsurface and surface *S*, where indirect *S* is lost from the stream network system (Buttle, 2016; Ehsanzedeh et al., 2012; Spence, 2010).

Although considerable, much of our understanding of the nonlinearity and threshold *P*–*R* responses of landscapes comes from regions with humid climates and studies concerning individual hillslopes (Redding & Devito, 2008), small catchments (Birkel et al., 2017; Peters et al., 1995; Saffarpour et al., 2016) or relatively homogenous, topographically driven, headwater catchments confined to local groundwater connectivity (Gannon et al., 2014; Julian & Gardner, 2014; Teutschbein et al., 2015). Temporal and spatial variations in catchment *S* to *R* relationships with alteration by shorter-term weather patterns such as seasonal *P* (snow accumulation, wet seasons) or intra-annual drying and wet cycles are well documented (e.g., Ali et al., 2015; Farrick & Branfireun, 2014; Saffarpour et al., 2016). The conceptualization and quantification of thresholds and lags from larger catchments with heterogeneous *S* properties and over longer temporal scales is still poorly understood (Carey et al., 2010; Tetzlaff et al., 2014) and can be highly variable across hydro-physio-climatic regions (Burn et al., 2008; Ross et al., 2021; Tetzlaff, Buttle, Carey, van Huijgevoort, et al., 2015; Zehe & Sivapalan, 2009).

The circumpolar Boreal is one of the world's largest and last contiguous forests and it plays an important role in the world's water and carbon cycles (Barr et al., 2012). Boreal forests also provide countless ecosystem functions and vast tracts of wildlife habitat (Smith & Reid, 2013). Recent circumpolar Boreal studies have increased our understanding of how variation in hydro-physio-climatic setting may influence catchment hydrologic functions and behavior across this important yet susceptible global ecosystem (Burn et al., 2008; Tetzlaff, Buttle, Carey, McGuire, et al., 2015). However, catchments with characteristics typical of continental glaciated plains regions of the boreal forest of North America and Eurasia have been conspicuously absent, limiting generalization and extrapolation of Boreal catchment hydrologic behavior.

In contrast to the relatively high relief of the Boreal Cordillera, and shallow soils and low permeable crystalline bedrock of the Boreal Precambrian shield, the hydro-physio-climatic setting of the Boreal Plains (BP) is characterized by low-relief, deep and heterogeneous surficial deposits, small long-term moisture deficits (potential evapotranspiration [*PET*]:*P* ratio ≤1), and low average regional *R* efficiency (<20% $RP^{-1}$; Buttle et al., 2000; Devito et al., 2005, 2017; Stralberg et al., 2020). Typical of continental plains (Právetz et al., 2015; Sun et al., 2020; Xu et al., 2011), large resistance of outflow to *P* inputs, nonlinearity, and spatial variability in catchment responses are expected due to the low relief and the predominance of vertical and subsurface exchange (Dreps et al., 2014; Klaus et al., 2015; Winter et al., 2003). Furthermore, continental regions with mean annual precipitation (MAP) within 10% of *PET* can experience large shifts in *R* with small interannual differences in *P* and *PET* (Jackson et al., 2009; Pilgrim et al., 1988; Zhou et al., 2015). On the other hand, the climate in the BP exhibits different periods of weather cycles, where annual *P* oscillates from below normal (drier) to near normal *P* over a 4–8-year period. This cycle is punctuated with 1 or 2 years of relatively large atmospheric moisture excess (*P* > *PET*) on roughly a 25-year period (Carrera-Hernández et al., 2011; Mwale et al., 2009). Similar to other systems across the continental Great Plains of North America (Mwale et al., 2011; Wolfe et al., 2019), the interaction of deep water storage with short- and long-term weather patterns has been shown to result in large spatial variability, strong thresholds, and hysteretic patterns in *S* to *R* relationships on selected catchments on the BP (Devito et al., 2005; Holecek, 1988; Wells et al., 2017). Addressing ecosystem service concerns and environmental flow needs requires a firm understanding of the controls on the natural range of seasonal and annual *R* generation. Such knowledge can reduce water security concerns by improving predictions of impacts from climate and land-use changes on both low and high annual flows, thus reducing uncertainty in water management decision making (Basu et al., 2020; Peters et al., 2022; Powell et al., 2017).

Despite the recognized complexity and spatial variability of landscape attributes, variability in hydrologic function has been broadly defined across the BP (Bridge & Johnson, 2000; Devito et al., 2005, 2012; Hokanson et al., 2019; Ireson et al., 2015; Smerdon et al., 2009) and similar ecohydrologic regions (Schoeneberger & Wysocki, 2005; van der Kamp & Hayashi, 2009; Winter et al., 2003) by considering the spatial heterogeneity of surficial glacial geology (i.e., fine- and coarse-textured deposits) that influences surface and subsurface *S* and hydrologic connectivity, as well as vegetation communities and water demands. The Boreal and Taiga Plains

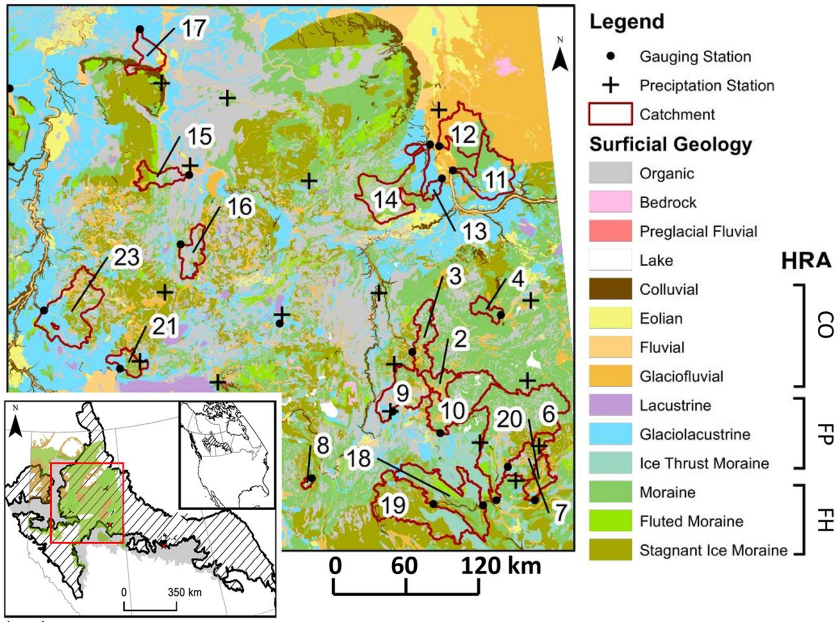


**Figure 1.** The distribution of river gauging sites (see Table 1 for the catchment identification [CID]), catchment boundaries, and precipitation gauging stations on surficial geology map (Fenton et al., 2013) of the northern Alberta study area. Coverage of defined coarse-texture glaciated landform (CO), fine-textured hummock (FH), and fine-texture clay-rich till and lacustrine plains (Fine_Plain [FP]) defined as in Devito et al. (2017). Inset shows the Boreal Plains ecozone of Canada (hashed lines) and the Boreal Forest Alberta Natural Region (Natural Regions Committee, 2006) in green.

differ in land cover from most other Plains regions, wherein extensive peatland development can cover >50% of the landscape; thus, ecohydrologic processes and storage–threshold relationships specific to peatlands need to be considered in generalizing catchment *R* between and within hydro-climatic regions (Carrer et al., 2015; Devito et al., 2012, 2017; Gracz et al., 2015; MacCulloch & Whitfield, 2012). Conceptualizing and classifying the catchment hydrologic function across the BP requires an understanding of complex interactions between dynamic weather patterns and the subtle relief, moderate to poor regional drainage, spatially variable glacio-surficial geology, and the mosaic of land covers that characterize the BP (Devito et al., 2005; Ireson et al., 2015; Mwale et al., 2011).

The overall objective of this paper is to identify and also quantify general relationships between landscape structure and *R* patterns over broad scales that vary in local climate regimes and landscape attributes. Here, we examine how *P* input signals are modified by the integration of heterogeneities in internal *S* and flow path connectivity in northern, low-relief, glaciated, heterogeneous catchments that are water limited. We examine annual *R* over a 25-year wet to dry weather pattern of 20 meso-scale catchments with ranges in proportions of the dominant landform and land-cover characteristic of the BP in western Canada. Our goal is to determine (a) the intracatchment and intercatchment range in magnitude of annual *R*; (b) the potential for annual *R* threshold responses to annual *P* inputs; (c) how the proportional cover of the dominant landform and land cover may influence catchment *P*–*R* relationships; and (d) the interaction between landscape characteristics and dynamic weather patterns on the spatial variability in temporal variations of catchment *P*–*R* relationships. Improving our understanding of how weather patterns interact with BP landscape characteristics, and thus potential water *S* and flow paths, to influence spatiotemporal variability in catchment *P*–*R* relationships will better inform management practices that require assessing climate and land use impacts on critical flows in the globally important BP.

## 2. Study Area

The study area is located within the Central Mixedwood (CMw) subregion of the Boreal Forest Natural Ecoregion of northern Alberta (Natural Regions Committee, 2006), which overlaps with the western portion of the BP ecozone of Canada (Marshall et al., 1999; Figure 1). The delineation and characteristics of the ecophysiological regions, surficial geology, soils, and land cover are detailed in Devito et al. (2017). In brief, the climate is cold

**Table 1**
*Characteristics and Indices of the Study Catchments*

| Catchment | | | | HRA | | HU | | | | R | | $RP^{-1}$ | | | Median R (mm) EACMS | | | Median $RP^{-1}$ EACMS | | |
|---|---|---|---|---|---|---|---|---|---|---|---|---|---|---|---|---|---|---|---|---|
| CID | Type | Area (km$^2$) | Slope (°) | CO (%) | FH (%) | Peat_Sw (%) | Decid_Mw (%) | P (mm) | R (mm) | Max (mm) | Min (mm) | Max (mm) | Min (mm) | Month Max R | Dry | Mesic | Wet | Dry | Mesic | Wet |
| 18 | FH | 4,700 | 1.3 | 1 | 45 | 17 | 42 | 444 | 3 | 61 | 0 | 0.10 | 0.00 | 4 | 1 | 3 | 61 | 0.00 | 0.01 | 0.10 |
| 19 | FH | 2,496 | 1.3 | 1 | 63 | 21 | 47 | 448 | 5 | 69 | 0 | 0.11 | 0.00 | 5 | 2 | 6 | 69 | 0.01 | 0.02 | 0.11 |
| 20 | FH | 492 | 1.0 | 18 | 54 | 24 | 32 | 454 | 9 | 85 | 0 | 0.12 | 0.00 | 5 | 9 | 11 | 64 | 0.03 | 0.02 | 0.10 |
| 21 | FH_PT | 427 | 1.2 | 9 | 31 | 30 | 57 | 491 | 20 | 115 | 1 | 0.17 | 0.00 | 4 | 2 | 23 | 106 | 0.01 | 0.05 | 0.17 |
| 7 | FH_PT | 726 | 0.8 | 8 | 48 | 43 | 24 | 462 | 17 | 168 | 0 | 0.25 | 0.00 | 7 | 8 | 23 | 168 | 0.03 | 0.05 | 0.25 |
| 8 | FH_PT | 57 | 1.1 | 2 | 51 | 41 | 43 | 424 | 26 | 165 | 9 | 0.27 | 0.02 | 5 | 10 | 26 | 85 | 0.03 | 0.06 | 0.14 |
| 15 | FH_PT | 492 | 0.9 | 5 | 29 | 53 | 34 | 442 | 47 | 151 | 1 | 0.21 | 0.00 | 5 | 1 | 37 | 151 | 0.00 | 0.09 | 0.21 |
| 23 | DC | 1,968 | 0.8 | 6 | 13 | 20 | 39 | 489 | 28 | 182 | 3 | 0.28 | 0.01 | 4 | 5 | 34 | 182 | 0.01 | 0.06 | 0.28 |
| 13 | PEAT | 165 | 1.0 | 0 | 25 | 38 | 39 | 429 | 83 | 215 | 12 | 0.46 | 0.04 | 5 | 12 | 91 | 159 | 0.04 | 0.21 | 0.32 |
| 14 | PEAT | 5569 | 0.7 | 4 | 12 | 69 | 11 | 423 | 70 | 204 | 6 | 0.41 | 0.02 | 5 | 6 | 69 | 204 | 0.02 | 0.17 | 0.41 |
| 9 | PEAT | 1,120 | 0.8 | 14 | 10 | 61 | 21 | 473 | 65 | 269 | 11 | 0.38 | 0.02 | 6 | 35 | 70 | 258 | 0.09 | 0.15 | 0.36 |
| 16 | PEAT | 619 | 0.7 | 14 | 17 | 66 | 25 | 459 | 61 | 251 | 5 | 0.37 | 0.01 | 5 | 8 | 62 | 251 | 0.02 | 0.14 | 0.37 |
| 17 | PEAT | 582 | 1.3 | 23 | 2 | 53 | 35 | 484 | 56 | 239 | 14 | 0.34 | 0.04 | 5 | 25 | 79 | 192 | 0.06 | 0.16 | 0.25 |
| 6 | PEAT | 4,911 | 1.1 | 29 | 27 | 40 | 23 | 462 | 51 | 216 | 9 | 0.33 | 0.02 | 6 | 35 | 46 | 216 | 0.13 | 0.10 | 0.33 |
| 10 | CO_DC | 3,078 | 1.1 | 47 | 2 | 36 | 36 | 502 | 43 | 212 | 13 | 0.26 | 0.03 | 6 | 26 | 46 | 212 | 0.06 | 0.09 | 0.26 |
| 12 | CO_PT | 1,457 | 0.7 | 40 | 0 | 69 | 19 | 427 | 88 | 178 | 15 | 0.36 | 0.05 | 6 | 15 | 87 | 163 | 0.05 | 0.20 | 0.31 |
| 11 | CO_PT | 1,320 | 0.8 | 48 | 0 | 73 | 21 | 440 | 119 | 210 | 30 | 0.43 | 0.11 | 6 | 30 | 116 | 186 | 0.11 | 0.26 | 0.34 |
| 2 | CO_PT | 425 | 1.3 | 62 | 3 | 44 | 34 | 477 | 96 | 272 | 50 | 0.34 | 0.12 | 6 | 80 | 90 | 182 | 0.21 | 0.20 | 0.28 |
| 3 | CO_PT | 781 | 0.9 | 38 | 10 | 63 | 20 | 468 | 105 | 319 | 31 | 0.36 | 0.10 | 6 | 54 | 115 | 280 | 0.16 | 0.23 | 0.35 |
| 4 | CO_PT | 279 | 0.8 | 64 | 0 | 54 | 30 | 464 | 76 | 271 | 19 | 0.42 | 0.06 | 6 | 44 | 67 | 206 | 0.12 | 0.15 | 0.32 |

*Note.* Study catchment identification (CID) number, slope (°). Type of catchment is based on nodes generated in regression tree analyses (Figure 5). See Figure 1 for river gauging locations, catchment boundaries and see Table S1 in Supporting Information S1 for specific location, names, and identification of Water Survey of Canada (WSC) gauging stations. Hydrologic response areas (HRAs) from percent coverage of coarse-textured glacial (%CO) and fine hummocky moraine (%FH) landforms; hydrologic units (HUs) from percent land-cover characteristics of the study catchments for peatlands and swamps (%Peat_Sw) and deciduous and mixedwood forests (%Decid_Mw) as defined in Devito et al. (2017). Median annual catchment precipitation ($P$) and runoff ($R$) in mm calculated using years 1986–2010 from Alberta Agriculture and Forestry (2014) Sacramento Rain Gauge Station, and WSC (2013), respectively. Shown are maximum annual (Max) and minimum annual (Min) runoff ($R$) and runoff efficiency ($RP^{-1}$) for the study period. EACMS, estimated catchment antecedent moisture states; see text for definition and calculation of median $R$ and $RP^{-1}$ during DRY, MESIC, and WET catchment antecedent moisture states.

subhumid, with mean annual air temperatures of −1.0°C to 0.2°C, MAP of 478 to 495 mm, and annual *PET* ranging from 511 to 523 mm (Marshall et al., 1999; Natural Regions Committee, 2006; see Table S1 in Supporting Information S1). Precipitation during the growing season (May–August) represents about 60%–70% of the annual *P*, while snowfall only represents about 25%, on average. Runoff is characterized in most years by late spring or summer peak flows with minor peaks during spring snowmelt (Devito et al., 2005; Mwale et al., 2011).

The CMw has subtle relief (average slope less than 1.4° in the study catchments); with flat to undulating plains and hummocky uplands with Quaternary surficial deposits varying in thickness from 20 to 200 m over calcareous bedrock (MacCormack et al., 2015). The depth of surficial geology limits surface water interactions with underlying bedrock (Hokanson et al., 2019; Ireson et al., 2015). The surficial geology of the CMw is roughly equal portions of fine-textured glacio-lacustrine deposits, hummocky clay-rich glacial till moraines and ice-contact landforms, and coarse-textured glacio-fluvial and aeolian deposits (Fenton et al., 2013), with moraine deposits becoming coarse textured (e.g., sandy moraines) in the eastern part of Alberta (Devito et al., 2017; Natural Regions Committee, 2006). Devito et al. (2017) described three major hydrologic regions in the CMw of northern Alberta with characteristic relief, dominant glacial surficial geology, and soil-vegetation land cover. Topographically high regions located on the south and west fringes of the CMw are predominantly of fine-textured (carbonate-rich bedrock source) hummocky landforms, with greater cover of deciduous forests that represent areas with low annual *R* (15 ± 10 mm; 3% ± 2% of *P*). Proximal to these higher lands, regional glacial flooding resulted in low-relief, fine-textured landforms that are associated with expansive regions of peatlands (organic surficial geology unit in Figure 1) and higher observed median annual *R* (64 ± 12 mm; 14% ± 3% of *P*). The higher lands and moraines of the north-eastern portion of the CMw have the greatest median annual *R* (97 ± 16 mm; 21% ± 4% of *P*) and have coarser textured landforms because the glacial material was sourced from the nearby granitic bedrock-rich Precambrian shield (Natural Regions Committee, 2006).

## 3. Data and Methods

### 3.1. Climate and Catchment Runoff Characteristics

The 20 study catchments (50–5,000 $km^2$) that represent the variation in climate, land cover, surficial geology, and topography across the CMw region of central Alberta are described in Devito et al. (2017) (Figure 1 and Table 1). Each catchment is assigned a catchment identification (CID) number. The selected 25-year hydro-climatic record captures the full range of wet, dry, and mesic (near normal) climate patterns experienced in this region (Devito et al., 2005; Mwale et al., 2009). Monthly stream discharges ($m^3$ $month^{-1}$) from 1986 to 2010 were obtained from the Water Survey of Canada HYDAT database (Water Survey of Canada, 2013; Table S1 in Supporting Information S1) and gap filled for lack of winter flows and normalized into unit-area *R* (mm $month^{-1}$) using catchment drainage areas as described in Devito et al. (2017). Annual (water year) *R* (mm) was derived using monthly *R* summed from November to October. Annual *P* (mm) was determined by distance weighting between three to five of the closest Alberta Agriculture and Forestry Sacramento gauges (2014; alter shielded; measured twice per year; 1 April and 31 October) to produce a continuous 25-year *P* record (Devito et al., 2017). Annual runoff efficiency ($RP^{-1}$) was determined from the annual ratios of median *R* and *P*.

Long-term cumulative *P* was used to estimate catchment antecedent moisture. Previous studies have shown that soil moisture and water levels may be poorly correlated with annual atmospheric fluxes in the BP due to the strong effects of multiyear *S* surplus or deficits (Devito et al., 2005, 2012; Hokanson et al., 2021; Holecek, 1988). The 1–3-year cumulative departure from the median precipitation (CDMP) was determined from the sum of departure $Yr_{i+(i-1)}$ from 25-year median annual *P* (1986–2010) of each catchment (see also Hokanson et al., 2019; Winter, 2001). Overall, the 2YrCDMP provided the best correlation with *R* using all catchments and years grouped (Figure S1 in Supporting Information S1) or individual catchments (Figure S2 in Supporting Information S1) and was used to estimate catchment antecedent moisture state. Visual inspection of 2YrCDMP versus normal scores (Figure S3 in Supporting Information S1) indicates major breaks defining years when catchments are likely to have dry (2YrCDMP ≤ −200 mm), mesic (−50 mm ≤ 2YrCDMP ≤ 50 mm), or wet (2YrCDMP ≥ 200 mm) catchment antecedent moisture states. The estimated catchment antecedent moisture state for each year was designated and a median *R* and $RP^{-1}$ for all years with potential dry, mesic, or wet catchment antecedent moisture condition were calculated for each catchment.

### 3.2. Catchment Characteristics

For each catchment, the average slope in degrees was calculated using ESRI ArcGIS software, and the percent fine-textured (%Fine) and coarse-textured (%CO) glacial deposits, combined to 100% coverage of each catchment, were determined from Alberta Geological Survey surficial geology mapping (Fenton et al., 2013) as in Devito et al. (2017). Three hydrologic response area (HRA) classifications were defined from coverage of coarse glacial deposits (CO) HRA, and %Fine was subdivided into fine hummock (FH) and fine plain (FP; Table 1). The FH and FP HRAs were previously termed as hummocky moraine and clay-plain, respectively, in Devito et al. (2017). Moraine landforms with coarse-texture geomorphic modifiers, primarily in north-eastern Alberta, were designated as CO HRA. Hydrologic units (HUs) that represent distinct vegetation land-cover groups were estimated using 24 vegetation classes present in a remotely sensed (Landsat TM) Ducks Unlimited Enhanced Wetland Classification (DUC, 2011). These classes represent the dominant land covers of open-water and marsh (%Open_Mr), peatland and swamp wetlands (%Peat_Sw), and aspen and mixedwood forest (%Decid_Mw) as delineated in Devito et al. (2017).

Statistical analysis using 20 catchments requires parsimonious selection of catchment variables to reduce the potential for spurious correlations (Berges, 1997). Only two of the three defined glaciated landforms (%CO, %FH) were used in the analyses to avoid spurious correlations. Posited conceptualizations of the water cycle for this region (Devito et al., 2012; Ireson et al., 2015; Winter, 2001) as well as *R* (Devito et al., 2017), hydrogeologic (Hokanson et al., 2019), and modeling (Hokanson et al., 2021; Smerdon et al., 2007; Thompson et al., 2015) studies show that percent coverage of catchment coarse (%CO) and fine hummocky (%FH) HRA's and Peat_Sw and Decid-Mw HU's landscape characteristics greatly influence *R* and $RP^{-1}$ responses of catchments on the BP. The variable selection here is based on our a priori conceptual model described in Devito et al. (2012, 2017) (Table 1), where *S* and transmissivity properties are expected to vary among coarse- and fine-textured landforms (Winter, 2001), and with topology within fine-textured landforms. Differences in soil *S*, water use, promotion of surface saturation, and *R* are expected between deciduous forests and wetland portions of the catchments.

### 3.3. Catchment Attributes and *R* and $RP^{-1}$ Response

Spearman's rank correlation coefficients ($r_s$) were initially used to assess relationships of the influence of proportional cover of landform and land cover with (a) maximum and minimum *R* or $RP^{-1}$ and (b) median *R* or $RP^{-1}$ for each designated catchment antecedent moisture state (dry, mesic, and wet). Correlations between variables that include products (or ratios) or sums of the original variable (i.e., *R* or *P* vs. $RP^{-1}$) were not conducted due to potential spurious correlations (Berges, 1997). To avoid Type I errors associated with multiple comparisons, the appropriate Bonferroni correction was used to assess statistical significance (Dunn, 1961; McDonald, 2008), which was ranked as either significant if $p < 0.00625$ or strongly significant if $p < 0.00125$. Only correlations that were at least significant are reported. All descriptive statistics and comparative analyses were conducted using R 4.1.2 (R Core Team, 2021). Forward-selection stepwise linear regression was used to assess the most important catchment characteristics in predicting median *R* and $RP^{-1}$ for each catchment antecedent moisture state. The stepwise function in R 4.1.2 tools was used with an entry and exit *p*-value for predictor variables of 0.05 and 0.10, respectively, while simultaneously forcing predicted *R* and $RP^{-1}$ to be positive (Helsel & Hirsch, 1992).

### 3.4. Runoff Threshold Responses

Here, we operationally define the presence of temporal thresholds as a large change in magnitude or nonlinear relationship between *R* response and change in meteorological input that may be represented by typical diagnostic shape (i.e., hockey stick, gamma (exponential), sigmodal, and stepwise). We operationally define the spatial threshold response in *R* as a large change in the magnitude of annual *R* or a difference in the *P*–*R* relationship with proportional cover of a catchment attribute (HRA or HU). The potential presence of thresholds and basic shape of the relationships between annual *R* or $RP^{-1}$ with annual *P* or 1YrCDMP, 2YrCDMP, and 3YrCDMP for all study catchments, specific catchment types, and with changes in proportional coverage of selected catchment attributes were determined using a modified protocol described by Ross et al. (2021).

The range of models examined included parametric models in the curvefit (linear, power, exponential, and logistic), general additive model (GAM), nonparametric local regression (LOESS) models, and finally piecewise regression (PWR) in the segmented package (Muggeo, 2003; R Core Team, 2021). The models were compared to the simple linear regression model. The criterion to identify the best model fit is complicated by the fact that the adjusted coefficient of determination (adj-$R^2$), commonly used for goodness of fit of linear models (see also Ross et al., 2021), is not applicable to nonlinear models. Thus, assessment of goodness of fit was based on adj-$R^2$ or $r^2$ (pseudo $R^2$) of correlations of predicted versus observed observations of the model. A moderate fit (adj-$R^2$ or $r^2 > 0.45$) was required to keep the model. Visual observation of the predicted versus studentized residuals (SR, <3) was used to assess if the data support a particular relationship or model, given the range of model types. In comparing competing models, models with an Akaike information criterion (AIC) of more than two units below indicate the data supported that model (Ross et al., 2021). AIC could not be calculated for the LOESS models; the residual standard error (RSE) and visual assessment of SR plots and relative $r^2$ were used to compare with competing models.

All linear, piecewise, and nonlinear models with associated AIC, RSE or generalized cross-validation scores (GVC), adj-$R^2$ or $r^2$, and SR plots were determined within the curve-fitting software (R Core Team, 2021). No transformations of variables were conducted. Each scatter plot was fit initially using the nonparametric LOESS function with modest smoothing (span = 0.8) and used to assess potential shape and potential break points or threshold in the relationships. Initial break points for PWR were estimated from visual assessment of the LOESS fitted model.

The best model fit of the competing relationships of $P$, 1YrCDMP, 2YrCDMP, or 3YrCDMP with $R$ based on AIC was used to detect $P$–$R$ thresholds and further assess the importance of different cumulative precipitation periods for estimating catchment antecedent moisture condition for all catchments together and for individual catchment types.

### 3.5. Runoff Response, Catchment Attributes, and Weather Patterns

To determine the potential role of catchment attributes for generating different $P$–$R$ relationships that are representative of the BP (Devito et al., 2012, 2017; Ireson et al., 2015), a subset of catchment variables, selected a priori, was entered in the multivariate regression tree (MRT) to initially classify or define catchment types with similar proportions of HRA and HU, and annual $R$ and $RP^{-1}$ (Ma, 2018). The MRT analyses were conducted using "mvpart" (De'ath, 2014) and the tree was pruned based on the complexity parameter (CP) with the minimum cross-validation error ($X$-error). The proportional coverage of the catchment characteristics at each split in the RT was used to group catchments into types. Scatter plots of the annual $R$ from each catchment in a group versus each of 1YrCDMP, 2YrCDMP, and 3YrCDMP were used to assess the potential threshold relationships. Graphical analyses of quantile–quantile plot ($Q$–$P$ plots) of ranked annual 2YrCDMP and $R$ for each catchment type were used to compare and assess interaction of $P$ inputs with $S$ and the resulting magnitude and nonlinear catchment $R$ and $RP^{-1}$ response within each catchment group. The interaction of temporal and spatial threshold responses during specific annual meteorological conditions was evaluated from the scatter plots of the relationship between annual $R$ and $RP^{-1}$. These were viewed with respect to changes in the proportion of catchment characteristics during median dry, mesic, and wet catchment antecedent moisture state. The selection of the best model fit and potential threshold responses was determined using the criterion provided above.

## 4. Results and Discussion

### 4.1. Nonlinear and Interannual Variability in Catchment $P$–$R$ Response

The patterns in annual $P$ and $R$ of the catchments over the study period spanning 1986–2010 are shown in Figure 2. Atmospheric teleconnection in weather patterns resulted in periods (2–4 years in length) where annual $P$ alternated between slightly below and above the long-term median $P$ (Figure 2a). These shorter-term weather patterns were punctuated by a less frequent period with annual $P$ much greater (wet) and less (drought) than the median $P$, commonly observed in the continental climate of the glaciated plains of western Canada (Carrera-Hernández et al., 2011; Mwale et al., 2009; Thompson et al., 2017). Although large variability in $R$ was observed among catchments for individual years (to be discussed in the next section), there were no years where maximum $R$ and $RP^{-1}$ exceeded 350 mm and 0.5, respectively. In eight catchments, the maximum $R$ and $RP^{-1}$ did not exceed 200 mm and 0.3, respectively, during the study period. The low maximum $R$ and $RP^{-1}$ reflects the small difference between MAP and $PET$ and the control of $ET$ and large $S$ of the BP regions (Buttle et al., 2005; Devito

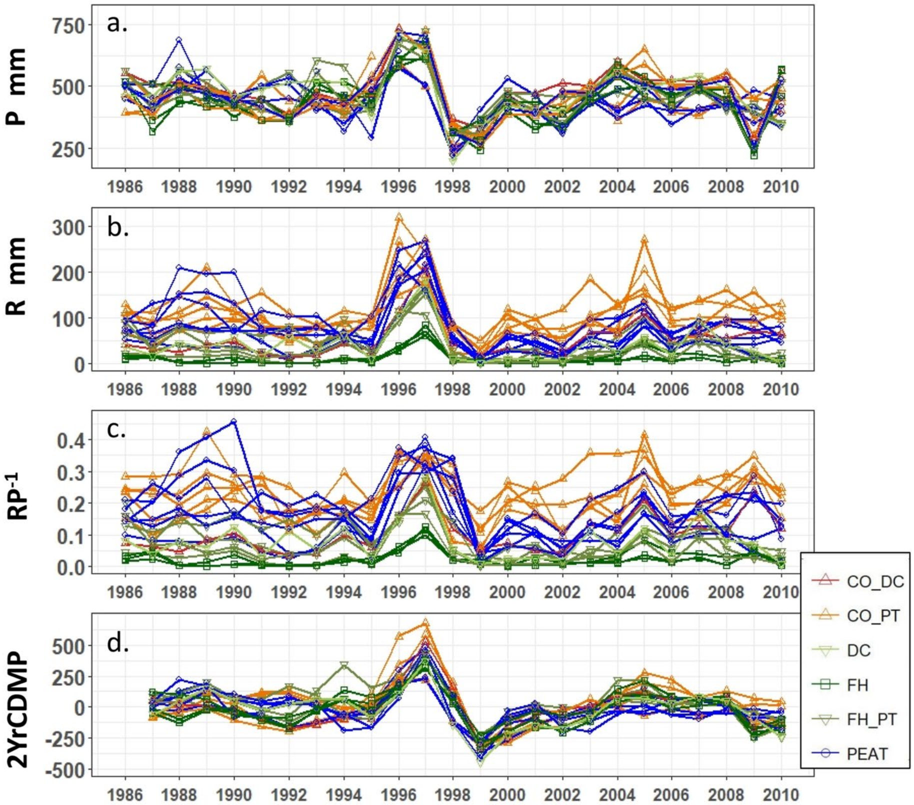


**Figure 2.** Time series (1986–2010) for annual (a) precipitation (*P* in mm), (b) runoff (*R* in mm), (c) runoff efficiency ($RP^{-1}$), and (d) 2-year cumulative departure from the long-term mean (2YrCDMP) in study catchments with type-defining dominant catchment characteristics (see Figure 5).

et al., 2017). Furthermore, annual *R* and $RP^{-1}$ varied by 2–3 orders of magnitude within individual catchments over the 25-year study period (Figures 2b and 2c).

Threshold responses in annual *R* to *P* are apparent across the study catchments (Figure 2). The threshold responses were also associated with lags in *R* response to the current year's *P*. This was most notable during the wetter 1996–1997 period and the drier 1998–1999 period, where catchments experienced greater and less than 200 mm (∼40%) departure from the long-term median *P*, respectively. Time lag and threshold *P*–*R* responses were also observed in several catchments in the late 1980s and 2005—2010. The lag and threshold responses resulted in poor relationships between annual *P* and *R* or $RP^{-1}$ across catchments, with greater than an order of magnitude difference in annual *R* from individual catchments observed between years receiving near normal *P* (Figure S1 in Supporting Information S1; see also Devito et al., 2005; Holecek, 1988).

Threshold responses were evident in all scatter plots using all years and catchments and plotting *R* against *P*, 1YrCDMP, 2YrCDMP, or 3YrCDMP. All nonlinear and PWR models evaluated showed an increase in model fit (adj-$R^2$) and a reduction in AIC of more than 20 when compared to the linear models for each scatter plot. The model comparison also indicated the importance of cumulative *P* for BP catchments generally. Comparisons of scatter plots using all years and catchments show that PWR models involving 2YrCDMP (Figure 3a) had the largest adj-$R^2$ (0.44) and lowest AIC (4,763) in predicting *R* compared to PWR models involving *P* (adj-$R^2$ = 0.37, AIC = 4,821), 1YrCDMP (adj-$R^2$ = 0.39, AIC = 4,808), or 3YrCDMP (adj-$R^2$ = 0.30, AIC = 4,870). Correlation analyses of individual catchments show a stronger relationship between annual *R* with the 2YrCDMP compared to annual *R* with annual *P* or 1YrCDMP for all but three study catchments (Figure S2 in Supporting Information S1).

These analyses show that, overall, the cumulative *P* over 2 years indicates the relative antecedent moisture status of most catchments on the BP (Devito et al., 2005; Holecek, 1988). Annual *P* relative to the median was

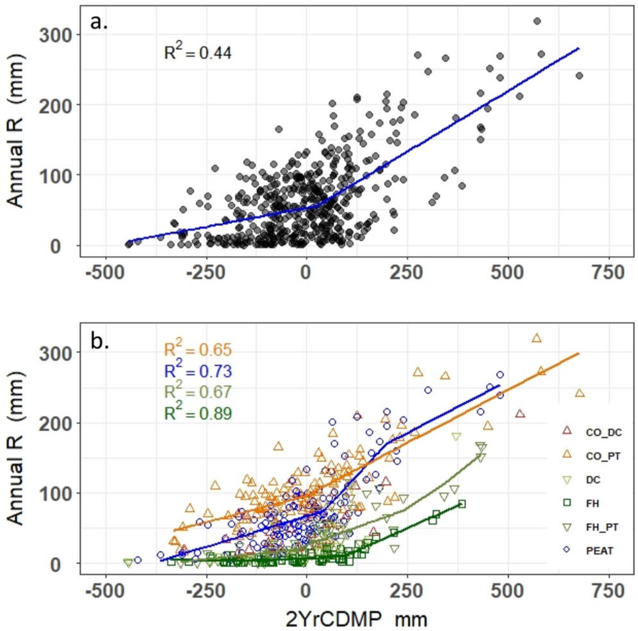


**Figure 3.** Annual runoff ($R$ mm) relative to the 2-year cumulative departure from the 25-year median annual precipitation (2YrCDMP) with adjusted $R^2$ and best model fit (piecewise regression) for (a) all study catchments and years and (b) individual relationships of the major catchment types (see Figure 5).

not consistent among catchments, precluding direct comparison of catchment moisture status by calendar year. Nonetheless, during 1996 and 1997, the maximum annual $P$ was observed in 1996 in many catchments, but the maximum annual $R$ and $RP^{-1}$ was primarily observed the following year. The 2YrCDMP was less than 200 mm in 1996 in most catchments, reflecting lower $P$ in the previous year. However, the 2YrCDMP was greater than 200 mm in most catchments during 1997, indicating wet antecedent conditions (Figure 2d). These results align with those of Peters et al. (2013) and Gibson et al. (2006) who found that a stronger relationship between annual $R$ and $P$ was achieved when the antecedent year $P$ was added to regression analyses for areas upstream of Great Slave Lake, which includes large extents of the BP generating runoff.

For all catchments, 1998 had the lowest annual $P$ observed during the study period and the previous 50 years (Carrera-Hernández et al., 2011), but the 2YrCDMP was moderate, annual $R$ was near the long-term median, and $RP^{-1}$ was generally high, reflecting the memory and $S$ of the previous wet years and lag in reduction of river flow during this very low $P$ year. The lowest annual $R$ and $RP^{-1}$ were observed in 1999 and again for most catchments in 2002, 1–4 years after the driest year in 1998 and corresponding to the lowest 2YrCDMP. Response times in $R$ to an increase to near normal $P$ from 2000 to 2005 varied from 1 to 4 years following the drought, with all catchments exhibiting increased $R$ and $RP^{-1}$ by 2004 and 2005. Additionally, individual catchments showed higher $RP^{-1}$ during dry years due to the lag in reduction of $R$ until the following years, such as for 2009.

Abrupt changes of threshold $P$–$R$ responses over time are expected in hydro-physio-climatic regions, such as the continental BP where the potential $S$ is large, due to the predominance of vertical flow in low-relief, deep glacial deposits with respect to relatively small differences (10%) in MAP and $PET$ (Jackson et al., 2009; Ross et al., 2021; Zhou et al., 2015). This study illustrates the importance of interactions between annual distribution of $P$ with catchment $S$ and antecedent condition (estimated catchment antecedent moisture) that can influence $R$ at meso-scale catchments across the BP of Alberta, resulting in orders of magnitude variation in $R$ or $RP^{-1}$ with average $P$, as observed in smaller headwater catchments on the BP (Devito et al., 2005; Holecek, 1988).

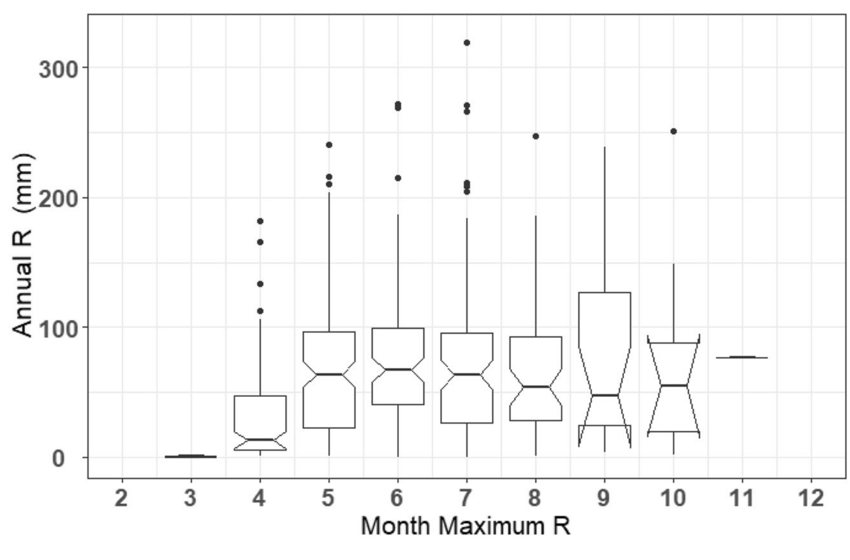


**Figure 4.** Annual runoff ($R$ mm) relative to the month with the maximum runoff ($R$) for that individual year for all study catchments.

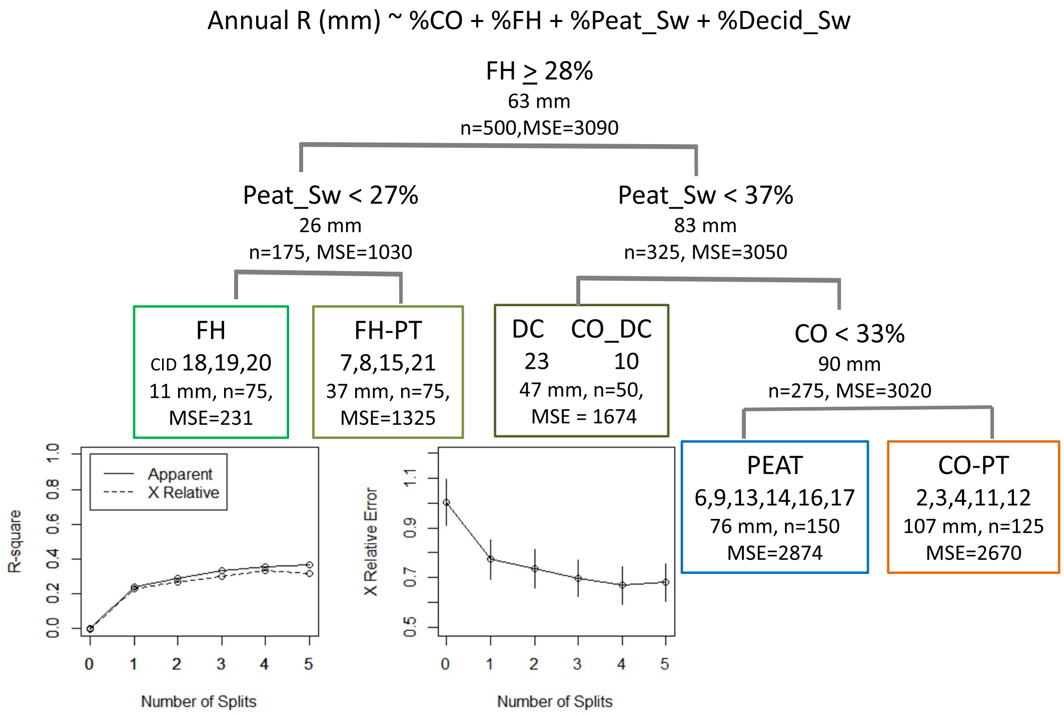


**Figure 5.** Multivariate regression tree (MRT) model predicting annual runoff (*R*) using dominant landforms (%FH, %CO) and land cover (%Peat_Sw, Decid_Mw). Sample size, *n* = 20 catchments with *n* = 500 annual *R*. Colored squares represent splitting and terminal nodes, respectively, and numbers within node symbols indicate group average runoff (mm) and sample size (*n*) for the listed catchments in each node. For conditions at each branch, move to the left.

The observed nonlinear *P*–*R* response and large interannual variability in *R* are further enhanced by the dominance of summer *P* in continental Boreal catchments. In this study, years with high magnitude *R* were associated with summer months experiencing large *R*. In contrast, years when spring melt dominated the seasonal flow, due largely to minimal summer *R*, the overall annual *R* was low (Figure 4). Although runoff efficiencies are generally greater following snowmelt, in contrast to snow-dominated regions, the overall contribution of snowmelt to annual *R* is low in the study catchments (Redding & Devito, 2010). Accumulation of snow water equivalent (CMw median = 120 mm) is low relative to potential soil and depression *S* (Redding & Devito, 2011), and there may also be considerable loss to groundwater recharge (Smerdon et al., 2008) resulting in minor snowmelt peaks in annual hydrographs in most years for BP catchments, as observed in summer *P*-dominated montane catchments (Goodbrand et al., 2022). Cyclonic summer patterns across the BP result in considerable range in magnitude, timing, and spacing of rain events, leading to dynamic antecedent moisture conditions that are synchronized with maximum rates of catchment *ET* (Devito et al., 2005; Mwale et al., 2011; Wells et al., 2017). Individual summer rain events large enough to exceed forest soil *S* are rare (Redding & Devito, 2008). Exceedance of soil *S* to generate *R* for extended periods is contingent on a cumulative surplus from multiple rain events, often from the previous years, particularly following extended dry periods where a memory of soil moisture *S* deficit can be substantial (Devito et al., 2005; Holecek, 1988).

Although the overall *R* generated is low, the expectation of potentially 2 orders of magnitude variability in *R* to a similar magnitude in annual *P* and the strong nonlinear response to the current year's *P* amount present challenges for anticipating and managing river flows. The observed relationship with 2YrCDMP is largely empirical but appears to represent an effective measure, albeit a coarse average, for determining antecedent moisture state for catchments in the BP. Application of 2YrCDMP or another cumulative climate index can aid in directing the timing of resource extraction activities to mitigate land use impacts on streams (Donnelly et al., 2016; Spafford & Devito, 2005), assessing long-term river flows for water security (Smerdon et al., 2009) or managing river and floodplain habitat (Peters et al., 2022) on the BP.

### 4.2. Catchment Characteristics and Runoff Relationships

#### 4.2.1. Contrasts in Catchment Characteristics

The large variability observed in annual $R$ and $RP^{-1}$ among catchments, in contrast to the variability in annual $P$ and 2YrCDMP, illustrates the large control of heterogeneity in catchment characteristics and $S$ on annual $R$ behavior (Figure 2 and Table 1). The MRT analyses of the four a priori selected catchment characteristics against annual $R$ produced four splits ($X$-error = 0.662, CP = 0.012) with a variable importance rank of FH (34%), Peat_Sw (24%), Decid_Mw (22%), and CO (20%; Figure 5). The sample size ($n$) and mean $R$ for each node provided in the MRT analyses correspond to the values for grouping of the specific catchment listed in each node. The proportional coverage of the catchment characteristics used at each split in the MRT provides a base for grouping catchments (see Table 1) on $R$ regime, and comparison of these groups provides insights into the type of catchment function and threshold responses.

Catchments with >28% FH (node 1) coverage had the lowest overall $R$ and $RP^{-1}$, representing seven catchments dominated by FH terrain (Table 1). Of these, $R$ was 3–4 times greater in catchments with >27% Peat_Sw cover. Thus, three catchments were classified as dominant FH, and the remaining four catchments with a combination of FH HRAs with considerable Peat_Sw HUs (FH_PT). The greatest overall $R$ and $RP^{-1}$ were observed in five catchments with >37% Peat_Sw (node 2) and >33% CO HRA coverage, labeled as CO_PT in Table 1. In six catchments with moderately high $R$, Peat_Sw was the dominant cover (PEAT). The two remaining catchments with lower FH and Peat_Sw coverage had a range of characteristics that did not readily fit into a catchment group, with CID 23 (DC) primarily dominated by Decid_Mw cover and CID 10 (CO_DC) with large %CO HRA and Decid_Mw coverage. For the following comparisons, CID 23 was included with the FH_PT catchment type and CID 10 with the CO_PT catchment type.

The four catchment types or groups depicted by the MRT (FH, DC, PEAT, and CO_PT) analyses are highlighted in Figure 2 and illustrate how similarities within and differences in proportion of $S$ and potential flow path can result in the large variability in $R$ versus $P$ observed across the study catchments (see also Figure S1 in Supporting Information S1). For all three individual catchment types dominated by fine-texture HRA, the overall goodness-of-fit increased by more than 10% and the AIC reduced by >27 for the range of linear and nonlinear models involving 2YrCDMP in predicting $R$ compared to the same models involving $P$, 1YrCDMP, or 3YrCDMP. In contrast, the $R$ versus cumulative $P$ relationships for CO_PT indicate similar fits for the range of model types for the scatter plots of annual $R$ involving 1YrCDMP and 2YRCDMP (Figure S4 in Supporting Information S1).

Best fit models of $R$ versus 2YrCDMP reveal the threshold magnitude, and relationships across each catchment type differ with the proportion of HRAs and HUs, from a more linear relationship in catchments with large %CO to a nonlinear and threshold relationship in catchments with poor drainage dominated with FH (Figure 3b). The PWR model with two or three break points was the best model fit for $R$ versus 2YrCDMP plots in the FT, FT_PT, and PEAT catchments, with a reduction in AIC > 27 and increase in the goodness-of-fit >8% compared to the simple linear model. The change in slope from the initial break points to the final was >10% in each model (Ross et al., 2021; Figure 3b). In contrast, the simple linear model for the $R$ versus 2YrCDMP plot of the CO_PT catchments could not be ruled out. There was only a modest reduction in AIC of 3.9 and increase in goodness-of-fit of 3%, and differences in slope of <3% (see Ross et al., 2021) when compared to the best fit PWR model with one break.

#### 4.2.2. Potential Storage of Catchment Types

Further detailed examination of $Q$–$P$ plot analyses for the catchment types illustrates the range in $S$–$R$ responses of the BP catchments (Figure 6). The $Q$–$P$ plots of the study catchments exhibit nonlinear responses with three distinct phases of catchment moisture state: (a) no or muted $R$ response to increased 2YrCDMP (driest), (b) slow and nonlinear rise in annual $R$ with increase in 2YrCDMP, and (c) larger and tending to linear increase with higher 2YrCDMP (wettest). The response of each catchment group differed in magnitude and extent of minimum annual $R$ in phase 1, and the value of 2YrCDMP in which phase 2 or 3 was initiated influenced the magnitude of $R$ during wetter conditions (e.g., 2YrCDMP at 200 mm; Figures 6a–6d).

The best fit PWR model relative to the simple linear model, estimated break points (psi1, psi2, psi3), and slopes (m1, m2, m3, m4) of the relationships between the break points are shown in Table 2 for the $Q$–$P$ plots for each catchment type shown in Figure 6. In the three FH catchments with FH > 45%, Decid_Mw > 30%, and with limited Peat_Sw coverage <25% (CID 18, 19, and 20), no or muted $R$ response ($m1$ = 0.007) was observed until the 2YrCDMP exceeded approximately −90 mm, which was followed by a slow rise in $R$ ($m2$ = 0.056) to about +80 mm 2YrCDM,

10.1029/2023WR034752

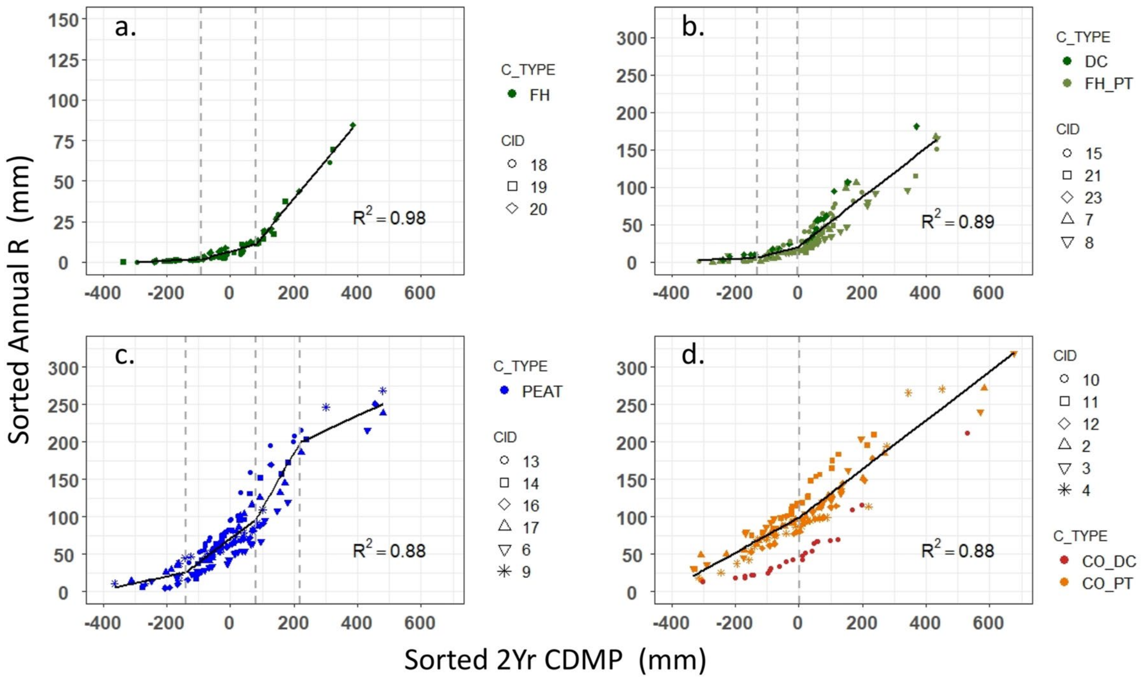


**Figure 6.** 2YrCDMP-runoff *Q–P* plots for the 20 study catchments designated into 4 catchment types (C_TYPE) based on regression tree analyses (see Figure 5). Note the different scale for (a) fine hummock (FH) catchment type. Numbers = catchment identification (CID; see Table 1). Shown is the best fit piecewise regression model for each catchment group, with estimated break points as dashed vertical lines. Catchment CID10 (CO_DC) was not included in piecewise regression (PWR) analyze of CO_PT.

after which there was a more rapid ($m3 = 0.236$) and linear increase with further increase in 2YrCDM. The average median annual $R$ of the three catchments was $11 \pm 3$ mm, the $R$ response to 2YrCDMP at 200 mm (wet catchment antecedent moisture state) was at or below 35 mm, and maximum $R$ was low, ranging from 60 to 90 mm.

FH_PT catchments (CID 7, 8, 15, and 21), characterized by >30% FH but with substantial %Peat_Sw coverage (>27%), were also associated with fine-textured HRAs with large coverage of aspen mixed forests (Table 1). Catchment CID 23 is plotted in this group due to the similar response. Although CID 23 has lower %FH (13%), it has substantial deciduous mixed forests in combination with fine-textured HRA which is associated with Peat_Sw coverage. The PWR analyses of the *Q–P* plots show threshold breaks with large changes in slope that vary in response among catchment types indicating contrasts in $S$ and surface connectivity with potential differences in

**Table 2**
*Best Fit Models for Q–P Plots of the Four Catchment Types in Figure 6*

| | Model | AIC | ΔAIC | RSE | $R^2$ | Adj-$R^2$ | Inter | $m1$ | psi1 | $m2$ | psi2 | $m3$ | psi3 | $m4$ |
|---|---|---|---|---|---|---|---|---|---|---|---|---|---|---|
| FH | PWR2 | 308 | −214 | 1.95 | 0.99 | 0.98 | 2.31 | 0.01 | −91.1 | 0.06 | 81.6 | 0.24 | | |
| | | | St. err | | | | 1.29 | 0.01 | 19.9 | 0.01 | 5.0 | 0.01 | | |
| FH_PT | PWR2 | 962 | −91 | 12.88 | 0.88 | 0.88 | 8.39 | 0.02 | −129.6 | 0.11 | −4.4 | 0.33 | | |
| | | | St. err | | | | 8.32 | 0.03 | 75.0 | 0.07 | 24.9 | 0.01 | | |
| PEAT | PWR3 | 1,274 | −59 | 19.52 | 0.88 | 0.88 | 38.91 | 0.09 | −140.6 | 0.32 | 81.3 | 0.75 | 218.5 | 0.20 |
| | | | St. err | | | | 13.79 | 0.06 | 35.6 | 0.04 | 20.6 | 0.12 | 27.9 | 0.06 |
| CO_PT | PRW1 | 1,043 | −5 | 18.23 | 0.88 | 0.88 | 99.14 | 0.23 | 3.1 | 0.33 | | | | |
| | | | St. err | | | | 3.71 | 0.03 | 53.7 | 0.02 | | | | |

*Note.* Piecewise regression (PWR) models with two or three breaks had the best fit for all four catchment types. Delta(Δ) Akaike information criterion (AIC) is PWR model AIC relative to the fitted linear model AIC, RSE, residual square error, and coefficient of determination ($R^2$) and adjusted $R^2$ (adj-$R^2$). Intercept (Inter) of the fitted model and estimated break points (psi) and slopes ($m$) of segments with standard errors (st. err).

configuration of FH landforms and Peat_Sw cover types (Figure 6). In contrast to FH class, $R > 5$ mm was initiated with lower 2YrCDMP (<−130 mm) values, followed by a low rate of increased $R$ ($m2 = 0.11$) when 2YrCDMP ranged from −130 mm to about 0 mm. This was then followed by a steeper and more linear rate of increasing $R$ ($m3 = 0.33$) in response to an increase in 2YrCDMP. The rate of increase in $R$ was greater than the FH group with larger 2YrCDMP. The median annual $R$ was 37 ± 8 mm and ranged from 75 to 125 mm at 2YrCDMP of 200 mm.

For PEAT catchments with a large proportion of Peat_Sw (>40%) and limited coverage of FH or CO HRAs (CID 6, 9, 13, 14, 16, and 17), the $Q$–$P$ plots overall show four phases (sigmodal like curve) of $R$ response. All catchments had some annual flow at the driest 2YrCDMP, albeit low (5–14 mm), with limited increase in $R$ ($m1 = 0.09$) with increase in 2YrCDMP to −140 mm. During more mesic periods, $R$ responses across PEAT catchments occurred in two steps, with a moderate increase in $R$ ($m2 = 0.32$) followed by a much steeper increases ($m3 = 0.75$) in $R$ at about −150 to 80 mm and then to 220 mm 2YrCDMP, respectively. Rates of increase appeared to reduce ($m4 = 0.20$) during the highest 2YrCDMPs. The average median $R$ for group PEAT was 76 ± 14 mm and annual $R$ at the wet antecedent moisture state (2YrCDM = 200 mm) were the highest (170–210 mm).

CO_PT catchments, with large portions of CO HRA (>33%) and extensive Peat_Sw coverage (>37%), show consistently greater annual $R$ (20–50 mm) during the driest conditions. In contrast to the other catchments, considerable increase in $R$ ($m1 = 0.23$) was observed during the lowest to about 0 mm 2YrCDM, followed by a modest increase of 10% in slope ($m2 = 0.33$) with higher 2YrCDMP. The linear increases in $R$ with 2YrCDMP were somewhat moderated compared to the PEAT catchments. Group CO_PT catchments had the greatest minimum flow and average median $R$ magnitude of 107 ± 12 mm, and ranged from 110 to 200 mm at wet 2YrCDMP of 200 mm. The CID 6 with 47% CO HRA but significant %FH and Decid_Mw coverage (group CO_DC) shows a nonlinear increase in $R$ with moisture states ranging from dry to mesic.

#### 4.2.3. Runoff Behavior and Catchment Types of the BP

The above analyses highlight the importance of classifying hydro-climatic catchment's $R$ response behaviors, not only globally (Wagener et al., 2007) but also within close geographical location with similar climate (Winter, 2001). Compared to other Boreal catchments, the role of BP catchments is largely to resist the transfer of $P$ to $R$. This functional trait of resistance (Carey et al., 2010) is due in part to the overall low relief, poor drainage efficiency, deep glacial deposits in conjunction with low annual $P$ that is similar in magnitude to the catchment $S$, and $PET$ (Ross et al., 2021). Although unexclusive, the $P$–$R$ responses of BP catchments also suggest that they have lower resilience—the ability of catchment $R$ to adjust to and/or recover from perturbations (Carey et al., 2010) when compared to other Boreal physiographic regions. This is indicated by the occurrence of thresholds in runoff responses to both drought and wet conditions in most catchments. However, although overall $R$ is low in the BP, there was a wide range in magnitude of $R$ and linearity in response that indicate differences in resistance and resilience functionality to interannual variability in $P$ of the study catchments. MRT classification and visualization of $Q$–$P$ plots identify commonalities or hydrogeologic response "type" of catchments that relate three major hydrologic regions in the CMw of central Alberta described by Devito et al. (2017). The interpretation of $Q$–$P$ plots is useful to further explore catchment groupings and functional relationships of traits (Carey et al., 2010; Ross et al., 2021) with respect to the potential type of drainage network and both active (i.e., short-term) and total $S$ (Devito et al., 2005; McNamara et al., 2011) that arise from the interaction of climate, relief, and deposition of the three dominant glaciated landforms (Eyles et al., 1999; Fenton et al., 2013) and provide further support for delineation of HRAs (Devito et al., 2005, 2017, Ireson et al., 2015; Winter, 2001).

Runoff regimes from catchments dominated with fine-textured HRAs (groups FH and FH_PT) provide an estimate of the relative influence of depression $S$ where a large fraction of $P$ is removed from regional $R$ by indirect $S$ and $ET$ (Ross et al., 2021). FH HRAs largely developed by stagnating ice during glaciation and large fields occur across the Boreal and Prairie Plains (Atkinson et al., 2014; Eyles et al., 1999). Deposition and irregularities in glacial ice-block melt processes produced large soil and depression $S$, in tandem with poor drainage networks. These factors result in the greatest resistance to transfer of $P$ to discharge of all catchment types. Measurable $R$ responses are limited to periods with large cumulative regional moisture surplus. These catchment types behave similar to low-relief, poorly drained continental Prairie and aspen Parkland catchments with limited effective catchment area, and threshold $R$ responses indicating "fill-and-spill" $R$ regimes, and long hydrologic memory of droughts (Ehsanzadeh et al., 2012; Mwale et al., 2011; Ross et al., 2021; Shaw et al., 2012). Extensive aspen forest coverage on the BP influences winter soil frost, reducing snow drifting and increasing snowmelt infiltration (Redding & Devito, 2008, 2011). This will further increase potential depression and surface $S$ and actual $ET$ by deep root uptake

(Hokanson et al., 2021), thereby further decoupling *R* responses to *P* and increasing the catchment resistance function (Carey et al., 2010) which results in lower magnitudes in maximum *R* when the "spill" thresholds occur.

In contrast to the Prairie systems, peatland coverage in cooler BP climate minimally covers ~20% of specific catchments and can exceed 50% even in fine-textured aspen-dominated hummocky terrain (Natural Regions Committee, 2006; Table 1). Peatland–aspen hillslope interactions at local scales (Hokanson et al., 2020) appear to counter some of the catchment *S* (i.e., Group FH_PT), decreasing resistance in the conversion of *P* to *R* as observed with lower *R* thresholds in catchments with large proportions of both FH and peatland coverage. The lower resistance to flow and threshold responses may result from both *R* responses in forest soils (Redding & Devito, 2008) and lower thresholds required for fill-and-spill responses with shallower peat filled depressions and peatland networks that have a more direct route to the catchment base. Nevertheless, catchments with large proportions of FH are clearly influenced by large total *S* and longer memory, enhanced by plant water uptake (Hokanson et al., 2021) in forest soils, that results in relatively high resistance to flow. Although not directly related, the high frequency of near zero flow years, large threshold behavior, and relatively inconsistent *P*–*R* relationships across years in functional response indicate that these catchments also have lower resilience to perturbations compared to catchments dominated with other landform types.

Decreased resistance to flow, in particular initiation of increased $RP^{-1}$ at lower moisture accumulation (2YrDMP < 100 mm), is observed in catchments dominated by fine plain HRAs and large peatland coverage (group PEAT). The increased response of *R* to *P* occurring at a lower threshold in cumulative *P* indicates that the overall *S* is smaller and the memory shorter, and thus the catchment resilience to weather patterns is greater compared to catchment dominated with hummocky terrain. Extensive peatlands formed in areas with deposits from actively flowing ice lobes and glacial-lacustrine regions that result in increased surface drainage over large regions of central Alberta (Atkinson et al., 2014; Eyles et al., 1999). The high water-holding capacity of peatland and swamp soils reduces active *S*, promoting near-surface saturation and *R* generation (Devito et al., 2017; Hokanson et al., 2021). Peatland development can further increase drainage networks and decrease resistance through increased terrestrialization of depressions (reduced *S*) and surface connections of larger areas by paludification (Hokanson et al., 2019). Furthermore, thermal properties of peat promote frost lenses that strongly limit *S* and result in decreased resistance, particularly during periods of snowmelt and late spring or early summer rain events (Petrone et al., 2008; Smerdon & Mendoza, 2010; Thompson et al., 2015). However, the observed threshold relationships indicate that lower peatland antecedent moisture in conjunction with low relief provides considerable *S* and resistance of *R* to *P* during drier periods of lower cumulative *P* and, likewise, may reduce catchment *R* resilience to drought conditions.

Catchments associated with large areas of glacio-fluvial plain landforms and coarse-textured moraines, typical of eastern Alberta (Atkinson et al., 2014; Devito et al., 2017; Natural Regions Committee, 2006), appear to have similarly lower resistances to flow. In contrast to fine-textured landforms, increased recharge and subsurface connection through deeper coarse deposits appear to increase base flow by adding to the drainage efficiency, resulting in the increased consistency of flow and extending flow during dry periods. In comparison with fine-textured catchments, where increased near-surface *S* may also lead to large water loss via *ET*, the increased role of snowmelt recharge (Carrera-Hernández et al., 2011; Smerdon et al., 2008) and dynamic *S* in groundwater in this hydro-climatic region increases the seasonality of *R* in response to *P* and appears to reduce resistance interannually (Buttle, 2016; Carey et al., 2010). The linear relationship between 2YrCDMP and annual *R* likely relates more to dynamic *S* and the time lag along subsurface flow path rather than exceeding indirect *S*, resulting in moderated response (higher resilience) to extremes in cumulative annual *P* and greater long-term runoff compared to fine-textured catchments dominated only with peatlands. The catchment *S* and *R* regimes in these catchments are similar to landscape interactions with lakes and streams observed in glacio-fluvial plains (Gibson et al., 2019; Hokanson et al., 2021; Winter et al., 2003) and coarse moraines across temperate and Boreal Canada (Buttle, 2016; Goodbrand et al., 2019; McNamara et al., 2011).

This analysis further corroborates the need for multiple conceptual hydrologic models for describing hydrologic behavior in continental BP by illustrating the importance of recognizing heterogeneity in geology. Distinguishing the roles played by fine- and coarse-textured landforms and topography on near-surface and subsurface flow, and on indirect and direct *S* on the plains landscape is key to understanding variability in catchment *R* (Devito et al., 2012; Winter, 2001). Combined with the previous long-term *R* analyses (Devito et al., 2017), this study also shows the importance of peatland distribution, formation and hydraulic properties in catchment *R* for continental Boreal regions as shown for other northern landscapes (Buttle et al., 2005; van der Velde et al., 2013).

**Table 3**
*Spearman Rank Correlation Matrix of Minimum and Maximum Annual Runoff (R) and Runoff Efficiency ($RP^{-1}$) Relative to Characteristics of the 20 Study Catchments*

| | $R$ (mm) | | $RP^{-1}$ | |
|---|---|---|---|---|
| | Min | Max | Min | Max |
| Slope | | | | |
| %CO | 0.79** | | 0.81** | |
| %FH | −0.62* | −0.76** | −0.65* | −0.74** |
| %Peat_Sw | | 0.67* | | 0.75** |
| %Decid_Mw | | | | −0.60* |

*Note.* Probability ($p$) values are adjusted using Bonferroni correction; *$p < 0.0125$ significant, **$p < 0.00625$ strongly significant. See Table 1 for definitions of acronyms.

This study not only shows that there is a large variation in long-term $R$ expected among catchments (Devito et al., 2017) but also reveals that large interannual variation in magnitude and threshold responses among neighboring headwater and mesoscale catchments should be expected in the BP. Care should be taken in generalizing $R$ across circumpolar Boreal landscapes as the order of magnitude or timing of $R$ observed in this study is not observed in catchments located in other Boreal physiographic regions (Ali et al., 2015; Tetzlaff, Buttle, Carey, McGuire, et al., 2015; Tetzlaff, Buttle, Carey, van Huijgevoort, et al., 2015). The landscape framework and catchment classes provided here and by Winter (2001), Devito et al. (2012, 2017), and Ireson et al. (2015), and catchment typologies presented in Ross et al. (2021), aid in extrapolating or scaling up catchment $R$. These contrasts in $R$ with HRA and HU likely explain a large portion of apparent contradiction observed in individual $R$ studies of smaller headwater catchments on the continental Boreal region (e.g., Devito et al., 2005; Holecek, 1988; Wells et al., 2017). Importantly, a large range in interannual low flow and frequency of drying should be expected for headwater to larger (fifth to sixth) order rivers, that must be considered in habitat management and water security (Peters et al., 2022) and, for example, the design, construction, and reclamation of landscapes (Devito et al., 2012; Ketcheson et al., 2016).

### 4.3. Shifts in Controls of Catchment Characteristics With Moisture State

Differences in the relationship of catchment HRA and HUs with minimum and maximum $R$ and $RP^{-1}$ indicate large temporal variability in the dominance of $R$ process and overall catchment hydrologic function within the BP. Considerable range in minimum $R$ (<0.1–50 mm) and $RP^{-1}$ (<0.01–0.11) was observed across catchments during the study period (Table 1). The relationship for catchment $R_{min}$ and $RP^{-1}_{min}$ showed a strong positive relationship with %CO (Table 3). In contrast, $R_{max}$ and $RP^{-1}_{max}$ were not significantly related to %CO, but rather the relationship shifted to a strong positive and negative relationship with Peat_Sw and FH coverage, respectively. $RP^{-1}_{max}$ were also negatively correlated to Decid_Mw cover.

The dominance of catchment properties and magnitude of influence on $R$ and $RP^{-1}$ differ, or shift, with changes in estimated catchment antecedent moisture. The median annual $R$ and $RP^{-1}$ from each catchment in a mesic antecedent moisture state (−50 > 2YrCDMP < 50 mm) ranged widely from 4 to 125 mm year$^{-1}$ and 0.01 to 0.26, respectively (Table 1). With a shift from dry to mesic estimated catchment antecedent moisture states (and further wet states), the positive relationship between $R$ and $RP^{-1}$ with %CO drops and strong positive and negative correlations between %Peat_Sw and %FH cover, respectively, develop (Figure 7 and Figure S5 in Supporting Information S1). Responses of $R$ and $RP^{-1}$ linearly increase with increased %Peat_Sw during wetter periods. The relationship with FH decreases exponentially with little influence on catchment $R$ and $RP^{-1}$ with less than 20–30 %FH coverage. Based on stepwise regression analyses, the best predictor on catchment $R$ (AIC = −105, adj-$R^2$ = 0.61) and $RP^{-1}$ (AIC = −121.9, adj-$R^2$ = 0.67) shifts to %Peat_Sw and %FH during mesic catchment antecedent moisture states.

Although catchment $R$ and $RP^{-1}$ are greater during wet catchment antecedent moisture states, compared to mesic antecedent states, the linear relationship of Peat_Sw and step function in %FH with $R$ or $RP^{-1}$ observed during mesic states remains during wet states (Figure 7). However, all catchment parameters except %CO were correlated with catchment $R$ responses (Table 4). Interestingly, a significant negative relationship is observed between both catchment slope and %Decid-Mw during periods where the estimated catchment antecedent moisture is wet, while no significant relationship is observed during periods when catchment antecedent moisture is estimated to be mesic or dry. Clear parameter selection to predict $R$ or $RP^{-1}$ during wet catchment antecedent moisture states was difficult to ascertain using stepwise regression and a four-parameter model is indicated to predict catchment $R$ (AIC = 151, adj-$R^2$ = 0.55) and $RP^{-1}$ (AIC = −112, adj-$R^2$ = 0.58).

The control of weather patterns on how landscape characteristics influence $R$ generation in the BP hydro-physio-climatic region is large. A first-order control of %CO was statistically selected for minimum flow in the study catchments. Similar relationships have been found between low annual flows or summer baseflow and % coverage of sandy till in glacial deposition regions (Winter, 2001; Winter et al., 2003) and bedrock-controlled landscapes (Buttle & Eimers, 2009; Tague et al., 2008; Tetzlaff et al., 2009), respectively. The physiographic controls of

10.1029/2023WR034752

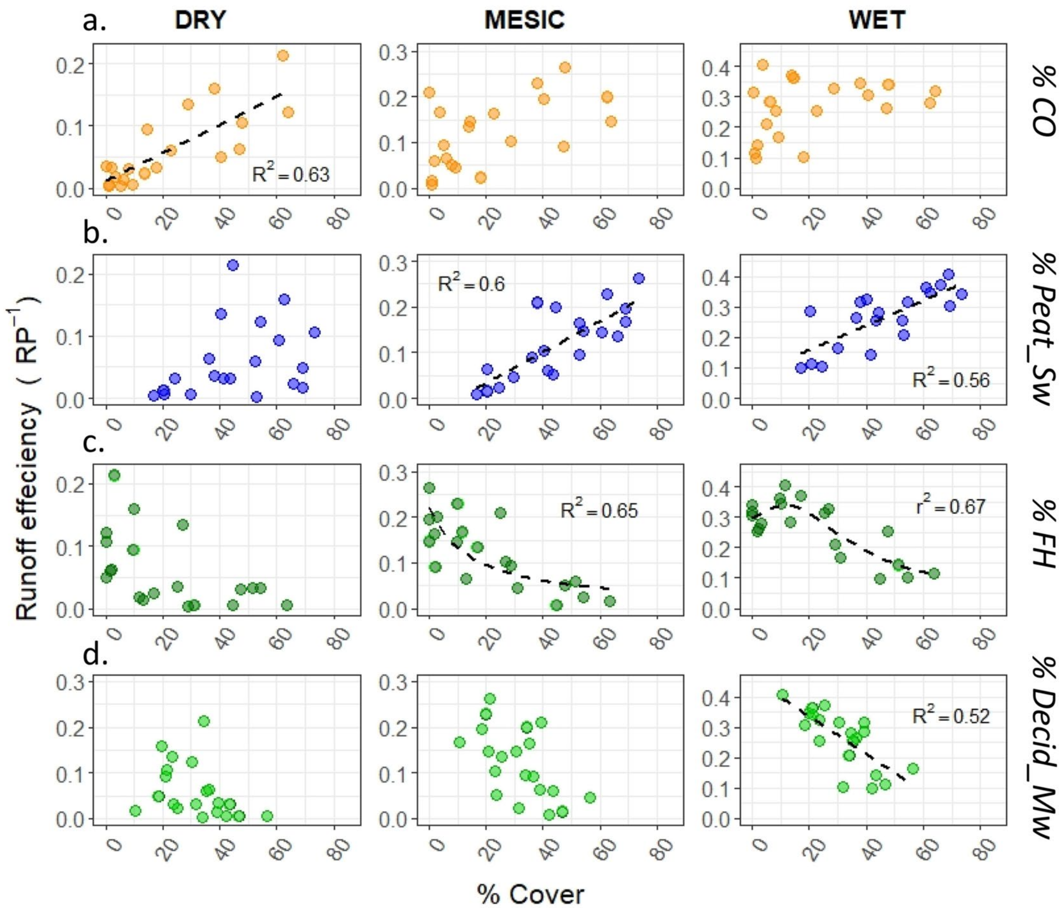


**Figure 7.** Pairwise comparison of median annual catchment runoff efficiency ($RP^{-1}$) during dry (2YrCDMP < −200 mm), mesic (−50 mm > 2YrCDMP > 50 mm), and wet (2YrCDMP > 200 mm) estimated catchment antecedent moisture states relative to % coverage of HRAs and HUs by row: (a) %CO (orange), (b) %Peat_Sw (blue), (c) %FH (dark green), and (d) %Decid_Mw (green). Best fit models shown as dashed line with adjusted coefficient of determination ($R^2$) or correlation of predicted versus observed ($r^2$).

coarse-textured landscapes for increased recharge and groundwater connectivity to main rivers occur during all climate cycles (Smerdon et al., 2008); however, their dominance in maintaining annual flow is expressed during periods of large moisture deficit. This study period represents some of the lowest flows of the century in the BP, and extended drought conditions have occurred with a 17 to 34-year periodicity (Carrera-Hernández et al., 2011; Mwale et al., 2009). Extreme low flows during droughts were associated with catchments dominated by fine

**Table 4**
*Spearman Rank Correlation Matrix of Median Annual R During Wet, Mesic, and Dry Moisture States and Percent Cover Characteristics of the 20 Study Catchments*

| | Median *R* (mm) moisture state | | | Median $RP^{-1}$ moisture state | | |
|---|---|---|---|---|---|---|
| | Dry | Mesic | Wet | Dry | Mesic | Wet |
| Slope | | | | | | −0.67* |
| %CO | 0.81** | | | 0.80** | | |
| %FH | | −0.80** | −0.75** | | −0.77** | −0.76** |
| %Peat_Sw | | 0.77** | 0.68** | | 0.79** | 0.76** |
| %Decid_Mw | | | −0.65* | | | −0.74** |

*Note.* Probability (*p*) values are adjusted using Bonferroni correction; $*p < 0.0125$ significant. $**p < 0.00625$ strongly significant. See Table 1 for definitions of acronyms.

texture with large areas of either FH and Decid_Mw or Peat_Sw land covers. A negative influence of FH is expected due to large indirect *S* and reduction of effective catchment area associated with poor surface connectivity (Devito et al., 2017; Ehsanzadeh et al., 2012). Feedbacks in peatlands, with their high holding capacity soils combined with their low relief, likely limit subsurface water movement to sustain baseflow during extended droughts in the BP, particularly compared to streams connected to coarse deposits (Thompson et al., 2017). This contrasts with the observed function of peatlands in sustaining stream flow during drought observed in higher gradient humid regions (Carrer et al., 2015; Flynn et al., 2021; Gracz et al., 2015); although humid Boreal regions are not likely to experience the cumulative moisture deficit experienced in this study on the BP.

The shift to dominant control of the interactions of Peat_Sw and FH cover on catchment *R* during mesic antecedent moisture conditions represents the average or normal long-term controls and conditions for BP catchments (Devito et al., 2017). The influence of Peat_Sw cover on catchment responses indicates the short-term memory of drought in peatlands due to lower effective soil *S*, reconnection of drainage networks, and near-surface contribution of peatlands to *R* that appear to overwhelm subsurface contributions from coarser deposits (Thompson et al., 2015). The concurrent negative relationship between *R* response and %FH reflects the longer memory of depression *S* of deciduous forest soils and poor drainage noted previously. Similar behavior has been observed in other Boreal hydro-physio-climatic regions where spatial integration of peat-dominated soils and well drained forest soils, with large contrast in *S* properties and water transmission, has been shown to influence the spatiotemporal variation in catchment *R* responses (Blumstock et al., 2016; Carrer et al., 2015; Karlsen et al., 2016; Tetzlaff et al., 2009).

The continuation of the interactive influence that Peat_Sw and FH have on maximum catchment *R* magnitude and $RP^{-1}$ during wet estimated antecedent moisture conditions on the BP was not expected. The influence of landscape heterogeneity on basin stormflow generally declines as event size increases (Buttle & Eimers, 2009) as various *S* components controlling *P*–*R* relationships are exceeded (Carrer et al., 2015), at least for humid, higher relief landscapes with shallower soils. In contrast, it is apparent that during wet years, regional scale *S* and long-term memory in forests and FH landforms can accommodate cumulative moisture inputs observed in the BP ecophysiographic subregion of the Boreal forest and continue to influence *P*–*R* relationships. Furthermore, although autocorrelated to some degree, the negative influence on higher *R* during wet years of deciduous forests, open-water wetlands, and slope associated with FH is manifested. This study also includes one of the wettest periods of the last century for this region (Carrera-Hernández et al., 2011; Smerdon et al., 2008; Thompson et al., 2017). Although infrequent, wet conditions offset dry periods, recurring every 17–34 years in northern Alberta (Mwale et al., 2009, 2011). Fine-textured hummocky moraines are ubiquitous at both the ecoregion (Figure 1; see also Devito et al., 2017; Eyles et al., 1999) and local scale (Hokanson et al., 2019) and it is apparent these landforms can influence *P*–*R* relationships in catchments during all regional moisture conditions (Devito et al., 2005; Holecek, 1988).

This intercatchment comparison is one of the first studies to illustrate how the role of landscape heterogeneity and the interaction of different *S* and connectivity on the nonlinearity of interannual *R* response and overall functional traits of catchments (McNamara et al., 2011) can shift dramatically with weather patterns, both within and between catchments in a physio-climatic region characteristic of the BP. The importance of longer-term oceanic patterns affecting continental weather oscillations and the interaction with shorter and local weather patterns on regional atmospheric moisture and response of catchment *R* has been long recognized (Basu et al., 2020; Mwale et al., 2011). However, the focus has largely been on intra-annual variability of *R* responses and timing of land use changes with teleconnection weather patterns of individual catchments (Goodbrand et al., 2022) or the variability between ecoregions, rather than comparing catchment responses within a region (MacCulloch & Whitfield, 2012).

Regions with subhumid climates (MAP within ±10% *PET*) respond proportionally greater to small changes in interannual *P* making catchment *R* particularly susceptible to alterations in land use and climate change (Cowood et al., 2017; Jackson et al., 2009). The interaction of subhumid climate and teleconnection weather patterns (Mwale et al., 2009, 2011) with heterogeneity in geology and land cover can result in large spatial and temporal variability in magnitude and threshold *R* response. Thus, large differences in catchment *R* behavior may be observed in neighboring catchments experiencing similar annual *PET* and *P* in the BP due to differences in antecedent moisture conditions with cumulative wet or dry periods. Quantifying and extrapolating the influence of variability in catchment characteristics and functional traits on *P*–*R* relationships on the BP requires a thorough understanding and quantification of regional weather patterns and the moisture state of the catchments prior to and during hydrologic observations. This study highlights and provides context for water-limiting and low-relief physiographic regions with overall large and variable system *S* and memory that are not well represented in intercatchment comparisons in developing catchment classifications (Bracken et al., 2013; Tetzlaff, Buttle, Carey, McGuire, et al., 2015), directing regional modeling (Faramarzi et al., 2015) and environmental management efforts at regional scales (Cowood et al., 2017; Klaus et al., 2015; G. Sun et al., 2011; Tetzlaff et al., 2010).

### 4.4. Circumpolar Catchment Runoff

The relatively large contrast in climate, geology, and relief across the circumpolar Boreal points toward a need to distinguish regions that are relevant to the scale of ecohydrological processes, management activities, land cover, and climate change (Ireson et al., 2015; Stalberg et al., 2022). The type and range of functional traits, low $RP^{-1}$, and intercatchment variability in threshold *P*–*R* responses observed in this BP intercatchment study were not captured in an intercomparison of near circumpolar northern catchments (i.e., North Watch) which included Cordilleran and Precambrian shield Boreal sites (Ali et al., 2015; Carey et al., 2010; Tetzlaff, Buttle, Carey, McGuire, et al., 2015; Tetzlaff, Buttle, Carey, van Huijgevoort, et al., 2015). These near circumpolar comparisons highlighted a range of *R*–*S* responses in catchments located primarily in humid snow-dominated climates, with relatively shallow soils or cooler regions dominated by permafrost. The BP represents about 25% of the total Boreal Forest in Canada, and with inclusion of the Taiga Plain, water-limited low-relief Plains regions represent over 40% of Boreal Canada. Physiographic regions similar to the BP in this study cover large areas of the Boreal in continental northern Eurasia (Binney et al., 2017). Such subhumid plains regions are susceptible to the cumulative effects of extensive land use, associated with energy (e.g., oil and gas) and forestry activities, fire disturbance, and climate change, leading to concerns for water allocation and long-term security of water resources (Ireson et al., 2015). Frameworks and catchment classifications for understanding and articulating the variability in catchment hydrologic function across the Boreal should distinguish regions with similar teleconnection weather patterns, geology, soils, and relief that have a large influence on catchment hydrologic *S* and memory (Klaus et al., 2015; Winter, 2001).

## 5. Conclusions

Generally, BP catchments strongly resist transfer of *P* to catchment *R* due to the nexus of relatively low *P* inputs, even during "wet" periods, low relief with poor drainage networks, large *S* capacity of glacial deposits, and the dominance of summer rainfall synchronized with forest growth. Runoff is low compared to other northern latitude hydro-physio-climatic regions (Buttle et al., 2005) and, thus, the wide array of *R* magnitude and threshold responses to interannual variability in *P* and magnitude of low and maximum flow associated with cumulative dry and wet moisture conditions observed in neighboring catchments have important implications for predicting and managing river ecohydrology. This intercatchment study supports current models for conceptualizing ecohydrologic interactions in continental glaciated landscapes where contrasts in fine- versus coarse-textured substrates and topology of glaciated landforms influence the type and magnitude of *S* and hydrologic connectivity within the catchments (Ireson et al., 2015; Smerdon et al., 2009; Winter, 2001). This study further introduces the importance of peatland and swamp land covers as source areas of *R* generation in contrast to deciduous forest's *S* control on catchment *R* behavior and function. Four general types of *R* behavior with cumulative *P* observed in this study were associated with landform and land-cover characteristic and catchment traits that are representative of the BP (Atkinson et al., 2014; Ireson et al., 2015; Natural Regions Committee, 2006) and other northern plains landscapes (Právetz et al., 2015; Schoeneberger & Wysocki, 2005; Winter, 2001; Zhou et al., 2015). The relationships and classification derived here could be used to estimate spatiotemporal variation in stream flow behavior of many continental and plains Boreal regions around the globe. These conceptual models are arguably more relevant to the scale of land-cover changes (e.g., mining, forestry, and wildfire) and better aid in directing land use and land reclamation management practices compared to those developed separately in smaller more homogenous catchments or from other physiographic regions of the Boreal.

## Data Availability Statement

The catchment land form and cover are provided in Table 1 and Table S1 in Supporting Information S1, as well as Devito et al. (2017). The basic river flow data can be downloaded from Water Survey of Canada HYDAT database (https://wateroffice.ec.gc.ca/) using the station identification numbers provided in Table S1 in Supporting Information S1. The annual runoff, cumulative departure from long-term precipitation median, geologic, and land-cover data used have been uploaded to www.Zenodo.org, link: https://doi.org/10.5281/zenodo.8361601.

**Acknowledgments**
We thank J. Morisette, K. Smith, and V. Hoyles from Ducks Unlimited Canada (DUC) for land-cover delineation; A. Anderson from Alberta Environment and Sustainable Resource Development for Sacramento precipitation data; and K. Pinder for help with GIS data collection on surficial geology. Thanks to Mika Little-Devito for help in navigating R code and programming. Funding was provided by the Boreal Program of DUC, Natural Sciences and Engineering Research Council-Collaborative Research and Development Grant (NSERC-CRDPJ477235-14) of Canada, and industry partners Syncrude Canada Ltd and Canadian Natural Resources Limited under Canada's Oil Sands Alliance grant (COSIA-LJ0215). Kerstin Stahl, Genevieve Ali, and two anonymous reviewers made valuable suggestions which improved the current manuscript.

## References

Alberta Agriculture and Forestry. (2014). Sacramento rain gauge stations. Retrieved from https://www.alberta.ca/fire-weather-and-forecasts.aspx

Ali, G., Tetzlaff, D., McDonnell, J. J., Soulsby, C., Carey, S., Laudon, H., et al. (2015). Comparison of threshold hydrologic response across northern catchments. *Hydrological Processes*, *29*(16), 3575–3591. https://doi.org/10.1002/hyp.10527

Atkinson, N., Utting, D. J., & Pawley, S. M. (2014). Landform signature of the Laurentide and Cordilleran ice sheets across Alberta during the last glaciation. *Canadian Journal of Earth Sciences*, *51*(12), 1067–1083. https://doi.org/10.1139/cjes-2014-0112

Barr, A. G., van der Kamp, G., Black, T. A., McCaughey, J. H., & Nesic, Z. (2012). Energy balance closure at the BERMS flux towers in relation to the water balance of the White Gull Creek watershed 1999–2009. *Agricultural and Forest Meteorology*, *153*, 3–13. https://doi.org/10.1016/j.agrformet.2011.05.017

Basu, S., Sauchyn, D. J., & Anis, M. R. (2020). Hydrological extremes in the Canadian Prairies in the last decade due to the ENSO teleconnection—A comparative case study using WRF. *Water*, *12*(11), 2970. https://doi.org/10.3390/w12112970

Berges, J. A. (1997). Ratios, regression statistics, and "spurious" correlations. *Limnology & Oceanography*, *42*(5), 1006–1007. https://doi.org/10.4319/lo.1997.42.5.1006

Binney, H., Edwards, M., Macias-Fauria, M., Lozhkin, A., Anderson, P., Kaplan, J., et al. (2017). Vegetation of Eurasia from the last glacial maximum to present: Key biogeographic patterns. *Quaternary Science Reviews*, *157*, 80–97. https://doi.org/10.1016/j.quascirev.2016.11.022

Birkel, C., Broder, T., & Biester, H. (2017). Nonlinear and threshold-dominated runoff generation controls DOC export in a small peat catchment. *Journal of Geophysical Research: Biogeosciences*, *122*, 498–513. https://doi.org/10.1002/2016JG003621

Blumstock, M., Tetzlaff, D., Dick, J. J., Nuetzmann, G., & Soulsby, C. (2016). Spatial organization of groundwater dynamics and streamflow response from different hydropedological units in a montane catchment. *Hydrological Processes*, *30*(21), 3735–3753. https://doi.org/10.1002/hyp.10848

Bracken, L. J., Wainwright, J., Ali, G. A., Tetzlaff, D., Smith, M. W., Reaney, S. M., & Roy, A. G. (2013). Concepts of hydrological connectivity: Research approaches, pathways and future agendas. *Earth-Science Reviews*, *119*, 17–34. https://doi.org/10.1016/j.earscirev.2013.02.001

Bridge, S. R. J., & Johnson, E. A. (2000). Geomorphic principles of terrain organization and vegetation gradients. *Journal of Vegetation Science*, *11*(1), 57–70. https://doi.org/10.2307/3236776

Burn, D. H., Buttle, J. M., Caissie, D., MacCulloch, G., Spence, C., & Stahl, K. (2008). The processes, patterns and impacts of low flows across Canada. *Canadian Water Resources Journal*, *33*(2), 107–124. https://doi.org/10.4296/cwrj3302107

Buttle, J. M. (2016). Dynamic storage: A potential metric of inter-basin differences in storage properties. *Hydrological Processes*, *30*(24), 4644–4653. https://doi.org/10.1002/hyp.10931

Buttle, J. M., Creed, I. F., & Moore, R. D. (2005). Advances in Canadian forest hydrology, 1999–2003. *Hydrological Processes*, *19*(1), 169–200. https://doi.org/10.1002/hyp.5773

Buttle, J. M., Creed, I. F., & Pomeroy, J. W. (2000). Advances in Canadian forest hydrology, 1995–1998. *Hydrological Processes*, *14*(9), 1551–1578. https://doi.org/10.1002/1099-1085(20000630)14:9<1551::AID-HYP74>3.0.CO;2-J

Buttle, J. M., & Eimers, M. C. (2009). Scaling and physiographic controls on streamflow behaviour on the Precambrian Shield, south-central Ontario. *Journal of Hydrology*, *374*(3–4), 360–372. https://doi.org/10.1016/j.jhydrol.2009.06.036

Carey, S. K., Tetzlaff, D., Seibert, J., Soulsby, C., Buttle, J., Laudon, H., et al. (2010). Inter-comparison of hydro-climatic regimes across northern catchments: Synchronicity, resistance and resilience. *Hydrological Processes*, *24*(24), 3591–3602. https://doi.org/10.1002/hyp.7880

Carrer, G. E., Rousseau, A. N., St-Hilaire, A., & Jutras, S. (2015). Mosaic surface storages of a small Boreal catchment. *Hydrological Processes*, *29*(6), 845–858. https://doi.org/10.1002/hyp.10195

Carrera-Hernández, J. J., Mendoza, C. A., Devito, K. J., Petrone, R. M., & Smerdon, B. D. (2011). Effects of aspen harvesting on groundwater recharge and water table dynamics in a subhumid climate. *Water Resources Research*, *47*, W05542. https://doi.org/10.1029/2010WR009684

Cowood, A. L., Moore, C. L., Cracknell, M. J., Young, J., Muller, R., Nicholson, A. T., et al. (2017). Expansion of landscape characterisation methods within the hydrogeological landscape framework: Application in the Australian Capital Territory. *Australian Journal of Earth Sciences*, *64*(8), 1073–1084. https://doi.org/10.1080/08120099.2017.1255656

De'ath, G. (2014). mvpart: Multivariate partitioning. R package version 1.6-2. Retrieved from https://CRAN.R-project.org/package=mvpart

Devito, K., Creed, I., Gan, T., Mendoza, C., Petrone, R., Silins, U., & Smerdon, B. (2005). A framework for broad-scale classification of hydrologic response units on the Boreal Plain: Is topography the last thing to consider? *Hydrological Processes*, *19*(8), 1705–1714. https://doi.org/10.1002/hyp.5881

Devito, K., Mendoza, C., & Qualizza, C. (2012). *Conceptualizing water movement in the Boreal Plains. Implications for watershed reconstruction*, *Synthesis report prepared for the Canadian Oil Sands Network for Research and Development* (p. 164). Environmental and Reclamation Research Group. https://doi.org/10.7939/R32J4H

Devito, K. J., Creed, I. F., & Fraser, C. J. D. (2005). Controls on runoff from a partially harvested aspen-forested headwater catchment, Boreal Plain, Canada. *Hydrological Processes*, *19*(1), 3–25. https://doi.org/10.1002/hyp.5776

Devito, K. J., Hokanson, K. J., Moore, P. A., Kettridge, N., Anderson, A. E., Chasmer, L., et al. (2017). Landscape controls on long-term runoff in subhumid heterogeneous Boreal Plains catchments. *Hydrological Processes*, *31*(15), 2737–2751. https://doi.org/10.1002/hyp.11213

Donnelly, M., Devito, K. J., Mendoza, C. A., Petrone, R., & Spafford, M. (2016). Al-Pac Catchment Experiment (ACE). *The Forestry Chronicle*, *92*(1), 23–26. https://doi.org/10.5558/tfc2016-007

Dreps, C., James, A. L., Sun, G., & Boggs, J. (2014). Water balances of two Piedmont headwater catchments: Implications for regional hydrologic landscape classification. *Journal of the American Water Resources Association*, *50*(4), 1063–1079. https://doi.org/10.1111/jawr.12173

Ducks Unlimited Canada (DUC). (2011). Enhanced wetland classification inferred products users guide version 1.0. Retrieved from http://www.ducks.ca.login.ezproxy.library.ualberta.ca/resources/industry/enhanced-wetland-classification-inferred-products-user-guide/

Dunn, O. J. (1961). Multiple comparisons among means. *Journal of the American Statistical Association*, *56*(293), 52–64. https://doi.org/10.1080/01621459.1961.10482090

Ehsanzadeh, E., Spence, C., van der Kamp, G., & McConkey, B. (2012). On the behaviour of dynamic contributing areas and flood frequency curves in North American Prairie watersheds. *Journal of Hydrology*, *414–415*, 364–373. https://doi.org/10.1016/j.jhydrol.2011.11.007

Eyles, N., Boyce, J. I., & Barendregt, R. W. (1999). Hummocky moraine: Sedimentary record of stagnant Laurentide Ice Sheet lobes resting on soft beds—Reply. *Sedimentary Geology*, *129*(1–2), 169–172.

Faramarzi, M., Srinivasan, R., Iravani, M., Bladon, K. D., Abbaspour, K. C., Zehnder, A. J. B., & Goss, G. G. (2015). Setting up a hydrological model of Alberta: Data discrimination analyses prior to calibration. *Environmental Modelling & Software*, *74*, 48–65. https://doi.org/10.1016/j.envsoft.2015.09.006

Farrick, K. K., & Branfireun, B. A. (2014). Soil water storage, rainfall and runoff relationships in a tropical dry forest catchment. *Water Resources Research*, *50*, 9236–9250. https://doi.org/10.1002/2014WR016045

Fenton, M. M., Waters, E. J., Pawley, S. M., Atkinson, N., Utting, D. J., & Mckay, K. (2013). *Surficial geology of Alberta (MAP 601 scale 1:1 000 000)*. Alberta Geological Survey. Retrieved from http://ags.aer.ca.login.ezproxy.library.ualberta.ca

Flynn, R., McVeigh, C., Mackin, F., & Wilson, F. R. (2021). Sources of stream base flow in blanket peat covered catchments. *Journal of Hydrology*, *603*, 126965. https://doi.org/10.1016/j.jhydrol.2021.126965

Gannon, J. P., Bailey, S. W., & McGuire, K. J. (2014). Organizing groundwater regimes and response thresholds by soils: A framework for understanding runoff generation in a headwater catchment. *Water Resources Research*, *50*, 8403–8419. https://doi.org/10.1002/2014WR015498

Gibson, J. J., Prowse, T. D., & Peters, D. L. (2006). Hydroclimatic controls on water balance and water level variability in Great Slave Lake. *Hydrological Processes*, *20*(19), 4155–4172. https://doi.org/10.1002/hyp.6424

Gibson, J. J., Yi, Y., & Birks, S. J. (2019). Isotopic tracing of hydrologic drivers including permafrost thaw status for lakes across Northeastern Alberta, Canada: A 16-year, 50-lake assessment. *Journal of Hydrology: Regional Studies*, *26*, 100643. https://doi.org/10.1016/j.ejrh.2019.100643

Goodbrand, A., Anderson, A., Devito, K., & Silins, U. (2022). Untangling harvest-streamflow responses in foothills conifer forests: Nexus of teleconnections, summer-dominated precipitation, and storage. *Hydrological Processes*, *36*(2), e14479. https://doi.org/10.1002/hyp.14479

Goodbrand, A., Westbrook, C. J., & van der Kamp, G. (2019). Hydrological functions of a peatland in a Boreal Plains catchment. *Hydrological Processes*, *33*(4), 562–574. https://doi.org/10.1002/hyp.13343

Gracz, M. B., Moffett, M. F., Siegel, D. I., & Glaser, P. H. (2015). Analyzing peatland discharge to streams in an Alaskan watershed: An integration of end-member mixing analysis and a water balance approach. *Journal of Hydrology*, *530*, 667–676. https://doi.org/10.1016/j.jhydrol.2015.09.072

Helsel, D. R., & Hirsch, R. M. (1992). *Statistical methods in water resources* (Vol. 49). Elsevier. https://doi.org/10.3133/twri04A3

Hokanson, K. J., Mendoza, C. A., & Devito, K. J. (2019). Interactions between regional climate, surficial geology, and topography: Characterizing shallow groundwater systems in subhumid, low-relief landscapes. *Water Resources Research*, *55*, 284–297. https://doi.org/10.1029/2018WR023934

Hokanson, K. J., Peterson, E. S., Devito, K. J., & Mendoza, C. A. (2020). Forestland-peatland hydrologic connectivity in water-limited environments: Hydraulic gradients often oppose topography. *Environmental Research Letters*, *15*(3), 034021. https://doi.org/10.1088/1748-9326/ab699a

Hokanson, K. J., Thompson, C., Devito, K., & Mendoza, C. A. (2021). Hummock-scale controls on groundwater recharge rates and the potential for developing local groundwater flow systems in water-limited environments. *Journal of Hydrology*, *603*, 126894. https://doi.org/10.1016/j.jhydrol.2021.126894

Holecek, G. (1988). Storage-effective drainage (SED) runoff model. *Journal of Hydrology*, *98*(3–4), 295–314. https://doi.org/10.1016/0022-1694(88)90019-4

Ireson, A. M., Barr, A. G., Johnstone, J. F., Mamet, S. D., van der Kamp, G., Whitfield, C. J., et al. (2015). The changing water cycle: The Boreal Plains ecozone of western Canada. *Wiley Interdisciplinary Reviews Water*, *2*(5), 505–521. https://doi.org/10.1002/wat2.1098

Jackson, R. B., Jobbagy, E. G., & Nosetto, M. D. (2009). Ecohydrology in a human-dominated landscape. *Ecohydrology*, *2*(3), 383–389. https://doi.org/10.1002/eco.81

Julian, J. P., & Gardner, R. H. (2014). Land cover effects on runoff patterns in eastern Piedmont (USA) watersheds. *Hydrological Processes*, *28*(3), 1525–1538. https://doi.org/10.1002/hyp.9692

Karlsen, R. H., Seibert, J., Grabs, T., Laudon, H., Blomkvist, P., & Bishop, K. (2016). The assumption of uniform specific discharge: Unsafe at any time? *Hydrological Processes*, *30*(21), 3978–3988. https://doi.org/10.1002/hyp.10877

Ketcheson, S. J., Price, J. S., Carey, S. K., Petrone, R. M., Mendoza, C. A., & Devito, K. J. (2016). Constructing fen peatlands in post-mining oil sands landscapes: Challenges and opportunities from a hydrological perspective. *Earth-Science Reviews*, *161*, 130–139. https://doi.org/10.1016/j.earscirev.2016.08.007

Klaus, J., McDonnell, J. J., Jackson, C. R., Du, E., & Griffiths, N. A. (2015). Where does streamwater come from in low-relief forested watersheds? A dual-isotope approach. *Hydrology and Earth System Sciences*, *19*(1), 125–135. https://doi.org/10.5194/hess-19-125-2015

Lin, H., Bouma, J., Pachepsky, Y., Western, A., Thompson, J., van Genuchten, R., et al. (2006). Hydropedology: Synergistic integration of pedology and hydrology. *Water Resources Research*, *42*, W05301. https://doi.org/10.1029/2005WR004085

Ma, X. (2018). *Using classification and regression trees: A practical primer*. Information Ages Publishing, Inc.

MacCormack, K. E., Atkinson, N., & Lyster, S. (2015). *Sediment thickness of Alberta, Canada. Alberta energy Regulator (AER/AGS Map 603, scale 1:1 000 000)*. Alberta Energy Regulator. Retrieved from http://www.ags.gov.ab.ca/publications/abstracts/MAP_603.html

MacCulloch, G., & Whitfield, P. H. H. (2012). Towards a stream classification system for the Canadian Prairie Provinces. *Canadian Water Resources Journal*, *37*(4), 311–332. https://doi.org/10.4296/cwrj2011-905

Marshall, I. B., Schut, P. H., & Ballard, M. (1999). *A national ecological framework for Canada: Attribute data*. Agriculture and Agri-Food Canada, Research Branch, Centre for Land and Biological Resources Research, and Environment Canada, State of the Environment Directorate, Ecozone Analysis Branch.

McDonald, J. H. (2008). *Handbook of biological statistics*. Sparky House Publishing. Retrieved from http://udel.edu/~mcdonald/HandbookBioStat.pdf

McNamara, J. P., Chandler, D., Seyfried, M., & Achet, S. (2005). Soil moisture states, lateral flow, and streamflow generation in a semi-arid, snowmelt-driven catchment. *Hydrological Processes*, *19*(20), 4023–4038. https://doi.org/10.1002/hyp.5869

McNamara, J. P., Tetzlaff, D., Bishop, K., Soulsby, C., Seyfried, M., Peters, N. E., et al. (2011). Storage as a metric of catchment comparison. *Hydrological Processes*, *25*(21), 3364–3371. https://doi.org/10.1002/hyp.8113

Muggeo, V. M. R. (2003). Estimating regression models with unknown break-points. *Statistics in Medicine*, *22*(19), 3055–3071. https://doi.org/10.1002/sim.1545

Mwale, D., Gan, T. Y., Devito, K., Mendoza, C., Silins, U., & Petrone, R. (2009). Precipitation variability and its relationship to hydrologic variability in Alberta. *Hydrological Processes*, *23*(21), 3040–3056. https://doi.org/10.1002/hyp.7415

Mwale, D., Gan, T. Y., Devito, K. J., Silins, U., Mendoza, C., & Petrone, R. (2011). Regionalization of runoff variability of Alberta, Canada, by wavelet, independent component, empirical orthogonal function, and geographical information system analyses. *Journal of Hydrologic Engineering*, *16*(2), 93–107. https://doi.org/10.1061/(ASCE)HE.1943-5584.0000284

Natural Regions Committee. (2006). *Natural regions and sub-regions of Alberta*. Compiled by D. J. Downing & W. W. Pettapiece; Pub. No. T/852. Government of Alberta.

Nippgen, F., McGlynn, B. L., Marshall, L. A., & Emanuel, R. E. (2011). Landscape structure and climate influences on hydrologic response. *Water Resources Research*, *47*, W12528. https://doi.org/10.1029/2011WR011161

O'Sullivan, A. M., Devito, K. J., Ogilvie, J., Linnansaari, T., Pronk, T., Allard, S., & Curry, R. A. (2020). Effects of topographic resolution and geologic setting on spatial statistical river temperature models. *Water Resources Research*, *56*, e2020WR028122. https://doi.org/10.1029/2020WR028122

Peters, D. L., Atkinson, D., Monk, W. A., Tenenbaum, D. E., & Baird, D. J. (2013). A multi-scale hydroclimatic analysis of runoff generation in the Athabasca River, western Canada. *Hydrological Processes*, *27*(13), 1915–1934. https://doi.org/10.1002/hyp.9699

Peters, D. L., Buttle, J. M., Taylor, C. H., & LaZerte, B. D. (1995). Runoff production in a forested, shallow soil Canadian Shield basin. *Water Resources Research*, *31*(5), 1291–1304. https://doi.org/10.1029/94WR03286

Peters, D. L., Watt, D., Devito, K., Monk, W. A., Shrestha, R. R., & Baird, D. J. (2022). Changes in geographical runoff generation in regions affected by climate and resource development: A case study of the Athabasca River. *Journal of Hydrology: Regional Studies*, *39*, 100981. https://doi.org/10.1016/j.ejrh.2021.100981

Petrone, R. M., Devito, K. J., Silins, U., Mendoza, C., Kaufman, S. C., & Price, J. S. (2008). Importance of seasonal frost to peat water storage: Western Boreal Plains, Canada.

Pfister, L., Martínez-Carreras, N., Hissler, C., Klaus, J., Carrer, G. E., Stewart, M. K., & McDonnell, J. J. (2017). Bedrock geology controls on catchment storage, mixing, and release: A comparative analysis of 16 nested catchments. *Hydrological Processes*, *31*(10), 1828–1845. https://doi.org/10.1002/hyp.11134

Pilgrim, D. H., Chapman, T. G., & Doran, D. G. (1988). Problems of rainfall-runoff modeling in arid and semiarid regions. *Hydrological Sciences Journal/Journal Des Sciences Hydrologiques*, *33*(4), 379–400. https://doi.org/10.1080/02626668809491261

Powell, N., Kløcker Larsen, R., de Bruin, A., Powell, S., & Elrick-Barr, C. (2017). Water security in times of climate change and Intractability: Reconciling conflict by transforming security concerns into equity concerns. *Water*, *9*(12), 934. https://doi.org/10.3390/w9120934

Právetz, T., Sipos, G., Benyhe, B., & Blanka, V. (2015). Modelling runoff on a small lowland catchment, Hungarian Great Plains. *Journal of Environmental Geography*, *8*(1–2), 49–58. https://doi.org/10.1515/jengeo-2015-0006

R Core Team. (2021). *R: A language and environment for statistical computing*. R Foundation for Statistical Computing. Retrieved from https://www.R-project.org/

Redding, T., & Devito, K. (2010). Mechanisms and pathways of lateral flow on aspen-forested, Luvisolic soils, Western Boreal Plains, Alberta, Canada. *Hydrological Processes*, *24*(21), 2995–3010. https://doi.org/10.1002/hyp.7710

Redding, T., & Devito, K. (2011). Aspect and soil textural controls on snowmelt runoff on forested Boreal Plain hillslopes. *Hydrology Research*, *42*(4), 250–267. https://doi.org/10.2166/nh.2011.162

Redding, T. E., & Devito, K. J. (2008). Lateral flow thresholds for aspen forested hillslopes on the Western Boreal Plain, Alberta, Canada. *Hydrological Processes*, *22*(21), 4287–4300. https://doi.org/10.1002/hyp.7038

Ross, C., Ali, G., Spence, C., & Courchesne, F. (2021). Evaluating the ubiquity of thresholds in rainfall-runoff response across contrasting environments. *Water Resources Research*, *57*, e2020WR027498. https://doi.org/10.1029/2020WR027498

Saffarpour, S., Western, A. W., Adams, R., & McDonnell, J. J. (2016). Multiple runoff processes and multiple thresholds control agricultural runoff generation. *Hydrology and Earth System Sciences*, *20*(11), 4525–4545. https://doi.org/10.5194/hess-20-4525-2016

Schoeneberger, P. J., & Wysocki, D. A. (2005). Hydrology of soils and deep regolith: A nexus between soil geography, ecosystems and land management. *Geoderma*, *126*(1–2), 117–128. https://doi.org/10.1016/j.geoderma.2004.11.010

Shaw, D. A., Vanderkamp, G., Conly, F. M., Pietroniro, A., & Martz, L. (2012). The fill–spill hydrology of Prairie wetland complexes during drought and deluge. *Hydrological Processes*, *26*(20), 3147–3156. https://doi.org/10.1002/hyp.8390

Singh, R., Archfield, S. A., & Wagener, T. (2014). Identifying dominant controls on hydrologic parameter transfer from gauged to ungauged catchments—A comparative hydrology approach. *Journal of Hydrology*, *517*, 985–996. https://doi.org/10.1016/j.jhydrol.2014.06.030

Smerdon, B. D., & Mendoza, C. A. (2010). Hysteretic freezing characteristics of riparian peatlands in the Western Boreal Forest of Canada. *Hydrological Processes*, *24*(8), 1027–1038. https://doi.org/10.1002/hyp.7544

Smerdon, B. D., Mendoza, C. A., & Devito, K. J. (2007). Simulations of fully coupled lake–groundwater exchange in a subhumid climate with an integrated hydrologic model. *Water Resources Research*, *43*, W01416. https://doi.org/10.1029/2006WR005137

Smerdon, B. D., Mendoza, C. A., & Devito, K. J. (2008). Influence of subhumid climate and water table depth on groundwater recharge in shallow outwash aquifers. *Water Resources Research*, *44*, W08427. https://doi.org/10.1029/2007WR005950

Smerdon, B. D., Redding, T. E., & Beckers, J. (2009). An overview of the effects of forest management on groundwater hydrology. *BC Journal of Ecosystems and Management*, *10*(1), 22–44.

Smith, K., & Reid, F. (2013). Spreading our wings in the Boreal. *Ducks Unlimited Canada Conservator*, Fall, 16–20.

Spafford, M., & Devito, K. J. (2005). *Boreal conservation: Hydrology and forestry in the Alberta-Pacific FMA area* (p. 24). Al-Pac White Paper. Alberta-Pacific Forest Industries Inc. Retrieved from https://open.alberta.ca/dataset/79bb8f5b-8c67-43a3-9d57-c1e8e97afe29/resource/d5a3eaaf-17ad-41ab-9ee2-4daa5fdb5385/download/srd-alpac-2005-forest-management-plan-appendix-3.pdf

Spence, C. (2010). A paradigm shift in hydrology: Storage thresholds across scales influence catchment runoff generation. *Geography Compass*, *4*(7), 819–833. https://doi.org/10.1111/j.1749-8198.2010.00341.x

Stralberg, D., Arseneault, D., Baltzer, J. L., Barber, Q. E., Bayne, E. M., Boulanger, Y., et al. (2020). Climate-change refugia in Boreal North America: What, where, and for how long? *Frontiers in Ecology and the Environment*, *18*(5), 261–270. https://doi.org/10.1002/fee.2188

Sun, G., Caldwell, P., Noormets, A., McNulty, S. G., Cohen, E., Myers, J. M., et al. (2011). Upscaling key ecosystem functions across the conterminous United States by a water-centric ecosystem model. *Journal of Geophysical Research*, *116*, G00J05. https://doi.org/10.1029/2010JG001573

Sun, J., Wang, X., & Shahid, S. (2020). Precipitation and runoff variation characteristics in typical regions of North China plain: A case study of Hengshui city. *Theoretical and Applied Climatology*, *142*(3–4), 971–985. https://doi.org/10.1007/s00704-020-03344-8

Tague, C., Grant, G., Farrell, M., Choate, J., & Jefferson, A. (2008). Deep groundwater mediates streamflow response to climate warming in the Oregon Cascades. *Climatic Change*, *86*(1–2), 189–210. https://doi.org/10.1007/s10584-007-9294-8

Tetzlaff, D., Birkel, C., Dick, J., Geris, J., & Soulsby, C. (2014). Storage dynamics in hydropedological units control hillslope connectivity, runoff generation, and the evolution of catchment transit time distributions. *Water Resources Research*, *50*, 969–985. https://doi.org/10.1002/2013WR014147

Tetzlaff, D., Buttle, J., Carey, S. K., McGuire, K., Laudon, H., & Soulsby, C. (2015). Tracer-based assessment of flow paths, storage and runoff generation in northern catchments: A review. *Hydrological Processes*, *29*(16), 3475–3490. https://doi.org/10.1002/hyp.10412

Tetzlaff, D., Buttle, J., Carey, S. K., van Huijgevoort, M. H. J., Laudon, H., McNamara, J. P., et al. (2015). A preliminary assessment of water partitioning and ecohydrological coupling in northern headwaters using stable isotopes and conceptual runoff models. *Hydrological Processes*, *29*(25), 5153–5173. https://doi.org/10.1002/hyp.10515

Tetzlaff, D., Carey, S. K., Laudon, H., & McGuire, K. (2010). Catchment processes and heterogeneity at multiple scales—Benchmarking observations, conceptualization and prediction. *Hydrological Processes*, *24*(16), 2203–2208. https://doi.org/10.1002/hyp.7784

10.1029/2023WR034752

Tetzlaff, D., Seibert, J., & Soulsby, C. (2009). Inter-catchment comparison to assess the influence of topography and soils on catchment transit times in a geomorphic province; the Cairngorm mountains, Scotland. *Hydrological Processes*, *23*(13), 1874–1886. https://doi.org/10.1002/hyp.7318

Teutschbein, C., Grabs, T., Karlsen, R. H., Laudon, H., & Bishop, K. (2015). Hydrological response to changing climate conditions: Spatial streamflow variability in the Boreal region. *Water Resources Research*, *51*, 9425–9446. https://doi.org/10.1002/2015WR017337

Thompson, C., Mendoza, C. A., & Devito, K. J. (2017). Potential influence of climate change on ecosystems within the Boreal Plains of Alberta. *Hydrological Processes*, *31*(11), 2110–2124. https://doi.org/10.1002/hyp.11183

Thompson, C., Mendoza, C. A., Devito, K. J., & Petrone, R. M. (2015). Climatic controls on groundwater-surface water interactions within the Boreal Plains of Alberta: Field observations and numerical simulations. *Journal of Hydrology*, *527*, 734–746. https://doi.org/10.1016/j.jhydrol.2015.05.027

van der Kamp, G., & Hayashi, M. (2009). Groundwater–wetland ecosystem interaction in the semiarid glaciated plains of North America. *Hydrogeology Journal*, *17*(1), 203–214. https://doi.org/10.1007/s10040-008-0367-1

van der Velde, Y., Lyon, S. W., & Destouni, G. (2013). Data-driven regionalization of river discharges and emergent land cover-evapotranspiration relationships across Sweden. *Journal of Geophysical Research: Atmospheres*, *118*, 2576–2587. https://doi.org/10.1002/jgrd.50224

Wagener, T., Sivapalan, M., Troch, P., & Woods, R. (2007). Catchment classification and hydrologic similarity. *Geography Compass*, *1*(4), 901–931. https://doi.org/10.1111/j.1749-8198.2007.00039.x

Water Survey of Canada. (2013). Hydrometric data (Vol. *2015*). Retrieved from https://www-ec-gc-ca

Wells, C., Ketcheson, S., & Price, J. (2017). Hydrology of a wetland-dominated headwater basin in the Boreal Plain, Alberta, Canada. *Journal of Hydrology*, *547*, 168–183. https://doi.org/10.1016/j.jhydrol.2017.01.052

Winter, T. C. (2001). The concept of hydrologic landscapes. *Journal of the American Water Resources Association*, *37*(2), 335–349. https://doi.org/10.1111/j.1752-1688.2001.tb00973.x

Winter, T. C., Rosenberry, D. O., & LaBaugh, J. W. (2003). Where does the ground water in small watersheds come from? *Ground Water*, *41*(7), 989–1000. https://doi.org/10.1111/j.1745-6584.2003.tb02440.x

Wolfe, J. D., Shook, K. R., Spence, C., & Whitfield, C. J. (2019). A watershed classification approach that looks beyond hydrology: Application to a semi-arid, agricultural region in Canada. *Hydrology and Earth System Sciences*, *23*(9), 3945–3967. https://doi.org/10.5194/hess-23-3945-2019

Xu, J., Chen, Y., Lu, F., Li, W., Zhang, L., & Hong, Y. (2011). The nonlinear trend of runoff and its response to climate change in the Aksu River, western China. *International Journal of Climatology*, *31*(5), 687–695. https://doi.org/10.1002/joc.2110

Zehe, E., & Sivapalan, M. (2009). Threshold behaviour in hydrological systems as (human) geo-ecosystems: Manifestations, controls, implications. *Hydrology and Earth System Sciences*, *13*(7), 1273–1297. https://doi.org/10.5194/hess-13-1273-2009

Zhou, G., Wei, X., Chen, X., Zhou, P., Liu, X., Xiao, Y., et al. (2015). Global pattern for the effect of climate and land cover on water yield. *Nature Communications*, *6*(1), 5918. https://doi.org/10.1038/ncomms6918